PAPER No. 389

Adaptation of Equiangular Spiral as an Open Channel Curve

By

KHALID MAHMOOD PSE I*

1. INTRODUCTION

Subcritical flow in open channel curves has the characteristic of potential separation from boundaries. Expanding flow, has a similar tendency, which worsens with the rate of expansion of the boundaries. If in any reach of an open channel, the two transitions are combined, it generally becomes difficult to prevent flow separation from the solid boundaries. Sound design practice therefore, requires that the transitions of expanding flow and curved flow may not be made contiguous.

Separation of flow from solid boundaries is objectionable on many counts. It creates undue concentrations within the cross section and in unlined channels, this can be the starting point of channel meandering. As the separated flow filaments are often unstable, the attack on the bed and banks may alternate from one side to the other, thereby increasing the extent of damage. In paved channels carrying sediment, shoals may be deposited in the dead zones which will vary in magnitude with the discharge and may thus lead to unsteady sediment load. The velocity distribution in the flow downstream of separation may also remain uneven over long stretches. The separation zones, indicate the presence of additional high shear planes and hence a greater loss of energy. The turbulence thus generated may travel for considerable distances downstream. Also from the aesthetic considerations, it seems necessary to design separation free channels and structures.

Qadirabad-Balloki Link, in its alignment would have crossed, Lower Chenab Canal (LCC) Upper at the former's R. D. 93 at an angle of 45°. This crossing would have been roughly 1,500 feet from the Sagar Regulator, where LCC Upper bifurcates into Upper Gugera Branch (UGB) and Lower Chenab Canal (LCC) Lower. The design discharge of the link at the crossing is 14,500 cusecs and that in LCC Upper a maximum of 12,000 cusecs. The full supply level in the link is about 11 feet below that of LCC Upper. From considerations

*Executive Engineer, Taunsa Barrage Division, Kot Adu, District Muzaffargarh.

of economics, structural stability, ease of construction etc., it was decided to provide a normal crossing between the two channels, with the LCC Upper passing through a RCC trough aqueduct over the link canal. The bed width of the aqueduct was maintained as 110 feet against the channel bed width of 240 feet. For providing a normal crossing, LCC Upper was relocated from R.D. 131 to Sagar Regulator, with two curves : one preceding the aqueduct with a radius of 5,000 feet and a deflection angle of about 45°, the other following the aqueduct with a centre line radius of 1,150 feet and a deflection angle of about 85°. The latter curve was made contiguous with the expansion transition downstream of the aqueduct.

The design of LCC Complex, which includes the relocation of LCC Upper from R.D. 131 to Sagar Regulator was referred to the Irrigation Research Institute for model studies on the aspects of silt charge distribution in the off-takes at Sagar Regulator and the hydraulic performance of the channel transitions downstream of the Aqueduct. These were studied on two different models at the Nandipur Field Research Station. The study of the hydraulic performance of the channel transition downstream of the Aqueduct showed that the design was inadequate as the flow through the curve suffered separation on both the banks in a major position of the 1150 feet radius curve. A number of devices were tried to improve the performance. These included longer expansion transitions, splitter vanes etc.; but were found inadequate. Finally, an equiangular spiral curve was designed between the end of the aqueduct and the relocated approach channel to Sagar Regulator. This combined expansion-*cum*-turning transition was found efficient, as it obviated separation from the solid boundaries and also ensured an even velocity distribution in the flow approaching Sagar Regulator.

This paper briefly describes the LCC Complex, the proposed design of the transitions downstream of the Aqueduct, their hydraulic behaviour as verified on the model and corrective devices tried on the model. It then gives the theoretical derivation of equiangular spiral as ideal fluid streamlines and some properties of the spiral. The method of fitting such a spiral to an actual problem is first discussed generally and is then followed by the design calculations adopted for the LCC Complex. The model and prototype performance of the spiral curve are also discussed. A brief discussion of the characteristics of open channel flow in bends is also included alongwith the limitations of theoretical analysis of this commonly experienced flow. It is hoped that this type of transition, which has proved successful, in the extremely critical imposed hydraulic conditions, will find use, when similar limitations are experienced elsewhere and the expansion and curve transitions are to be made contiguous.

2. ACKNOWLEDGEMENTS

The writer worked on the problems of LCC relocation etc.; during his tenure as Hydraulic Officer, in the Irrigation Research Institute during 1964-66. The design of the spiral was carried out by him. Malik Abdul Khaliq, Junior Research Officer, of the Institute worked on the construction and operation of the model and showed untiring devotion in the study of this and some other problems. His help is gratefully acknowledged. The data on the prototype velocity measurements were got observed by Mian Masud Ahmad, Deputy Project Director, Links WAPDA at the request of the writer. The actual observations were got made by the Surface Water Hydrology Directorate of WAPDA. The writer expresses his gratitude to Mian Masud Ahmad for this help.

3. L C C COMPLEX

A layout plan of Qadirabad-Balloki Link and Lower Chenab Canal Upper in the vicinity of their intersection is shown in Figure 3.1. The Complex, consists of the following works:

1. An Aqueduct structure to carry LCC Upper (12,000 cusecs) normally across Qadirabad-Balloki Link (14,500 cusecs).
2. A head regulator off-taking upstream of the crossing to supply LCC Feeder Canal for supplying Rakh and Jhang Branches of LCC system.
3. A regulation-*cum*-control structure in the link for possible future retrogression of the link.
4. Relocated LCC Upper from R. D. 131 to Sagar Regulator.

A number of alternatives were considered in the original Design Report (3.1)* and the proposed scheme with the following design data of the Aqueduct and the relocated LCC Upper was adopted.

(*i*) Qadirabad-Balloki Link

Normal capacity	: 14,500 cusecs.
Bed Width	: 300 feet.
Section	: unlined
Bed slope	: 1 in 7700
Bed level	: 676.3 ±
Full supply depth	: 12 feet

*Number in the parentheses refer to list of references given at the end of the text.

(*ii*) Relocated LCC Upper
Upstream of Aqueduct

Design discharge	: 8,000 cusecs
Maximum capacity	: 12,000 cusecs
Bed width	: 210 feet
Section	: unlined with outside bank lined on curve
Depth (8,000 cusecs/12,000 cusecs)	: 10.3/12.9 feet.
Bed slope	: 1 in 6250

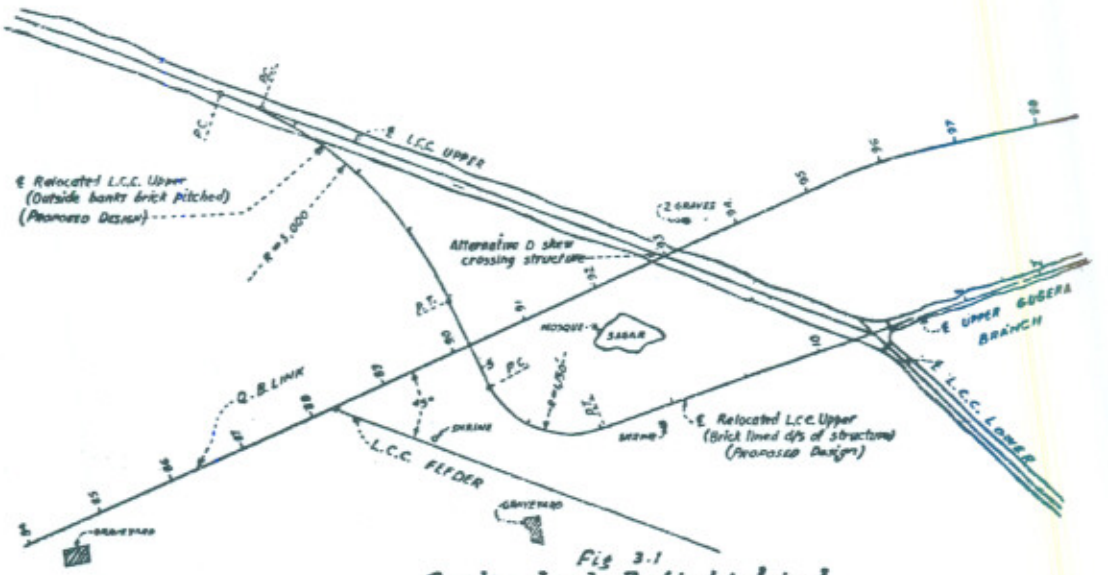

Fig 3.1
Qadirabad Balloki Link
and
Lower Chenab Canal Upper
in
the Vicinity of their intersection

Downstream of Aqueduct

Design discharge	: 8,000 cusecs
Maximum capacity	: 12,000 cusecs
Bed width	: 240 feet
Section	: Brick lined
Depth (8,000/12,000 cusecs)	: 10.0/12.78 feet
Bed slope	: 1 in 11100

Channel Curve Upstream

Curve	: Right handed
Centre line radius	: 5,000 feet
Deflection angle	: 45°—06′—20″
P. C.	: RD 131+101.09
P. T.	: RD 135+065.89

Channel Curve Downstream

Curve	: Left handed
Centre line radius	: 1,150 feet
Deflection angle	: 85°—16′—10″
P. C.	: RD 136+310.84
P. T.	: RD 138+022.30

(*iii*) Aqueduct

Crossing with Q. B. Link	: Normal
Design discharge	: 8,000 cusecs
Maximum capacity (with no free board)	: 12,000 cusecs
Bed width	: 110 feet
Depth (8,000 cusecs)	: 9.5 ft. to 9.2 ft.
Depth (12,000 cusecs)	: 11.8 ft. to 11.4 ft.
Bed level	: 690.5
Water surface level (8,000 cusecs)	: 700.0 to 699.7
Water surface level (12,000 cusecs)	: 702.3 to 701.9

The plot plan showing the layout of the Link, existing LCC Upper and proposed relocation up to Sagar Regulator is shown in Figure 3.2. The proposed inlet and outlet transitions for the aqueduct are shown in Figure 3.3. It may be seen that the outlet transition consists of 494 feet radius circular arcs, expanding the bed width from 110 feet to 240 feet and flattening the side slope from vertical to 2 : 1 in a length of 260 feet. On the inlet transition the bed width is contracted from 210 feet to 110 feet in a length of 181 feet through single circular arcs of 285 feet radius. The downstream and upstream transitions provide flaring out and flaring in of 1 in 4 and 1 in 3.6 respectively.

The hydraulic elements of the flow in the channel upstream of the aqueduct in the aqueduct and in the channel downstream of the aqueduct are given in Table 3.1. It may be seen that a flaring out of 1 in 4 from Froude number of 0.50 to 0.18 and bed width of 110 feet to 240 feet is sufficiently inadequate. The curve in the downstream channel with a radius-width ratio of 4.8 is also inadequate and would suffer from serious inequality of velocities if not separation. In the Irrigation Department, the limiting channel radii are related to discharges and since the channel dimensions generally conform to Lacey's empirical equations, the radii can be related to the channel dimensions. The minimum radii for unlined canals are generally specified as 20 to 35 times the wetted parameter with a minimum of 5,000 feet for channel above 3,000 cusecs capacity.

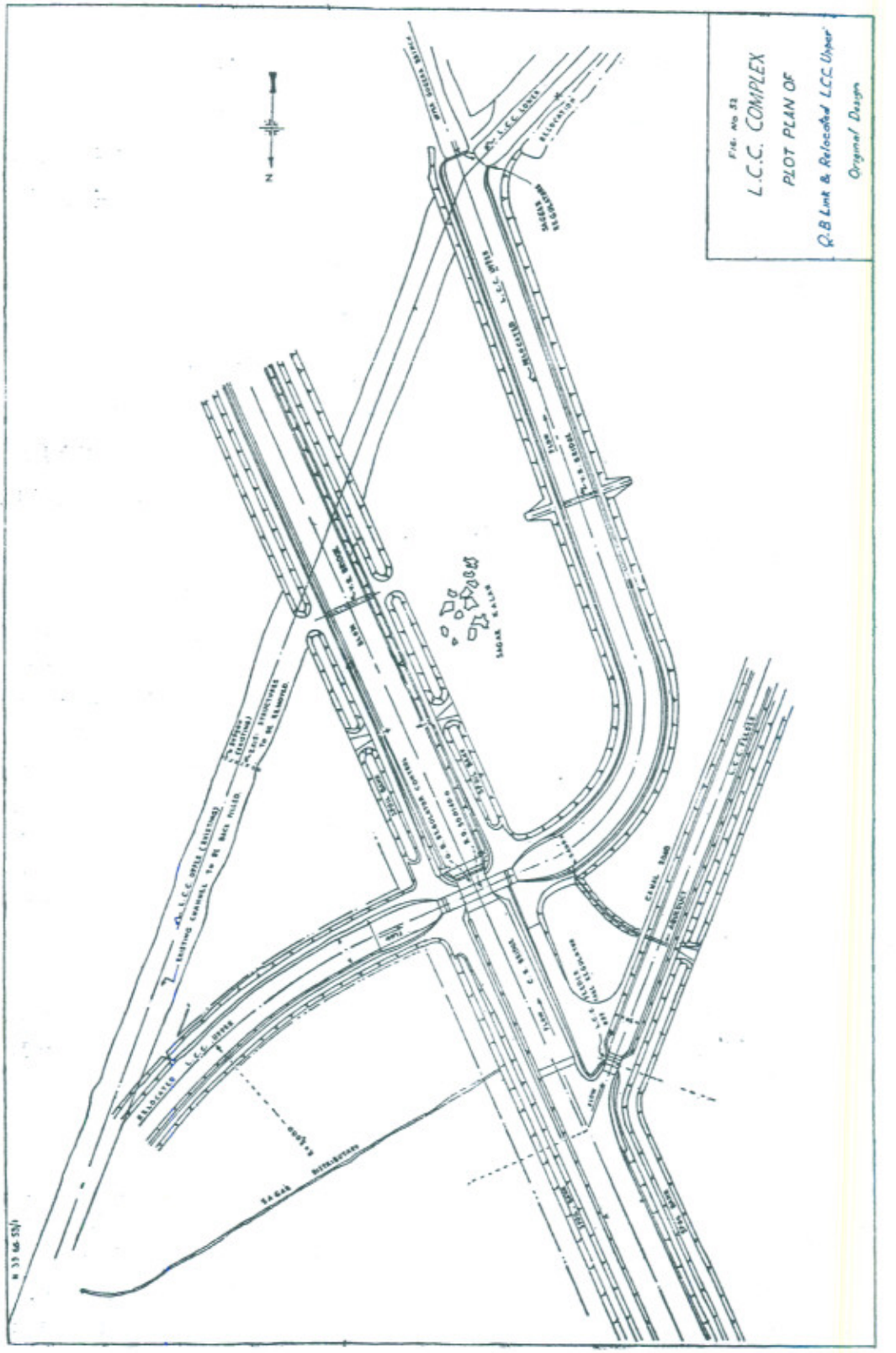
L.C.C. COMPLEX
PLOT PLAN OF
Q.B Link & Relocated L.C.C Under
Original Design

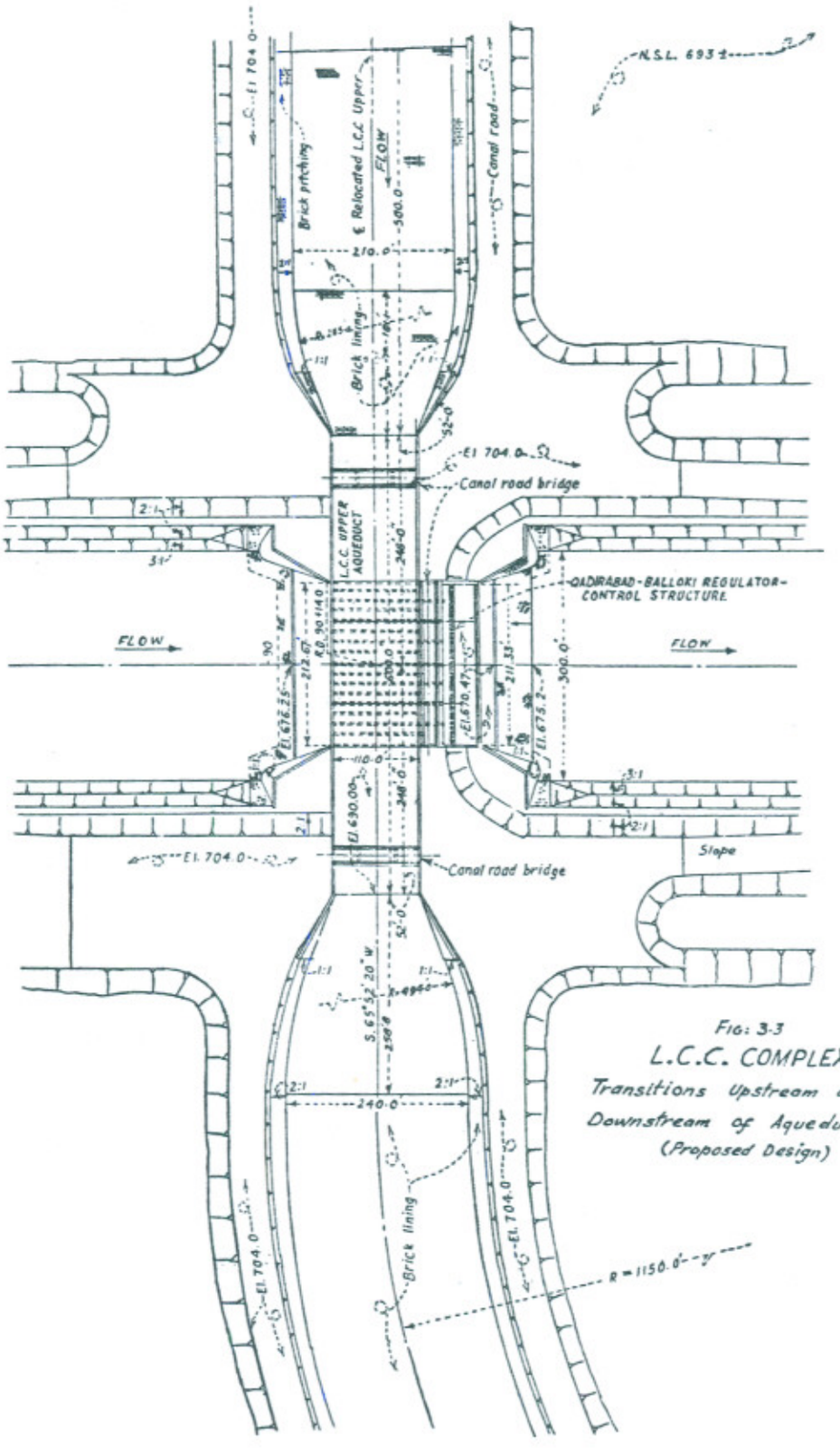

FIG: 3-3
L.C.C. COMPLEX
Transitions Upstream and Downstream of Aqueduct
(Proposed Design)

TABLE 3.1

Hydraulic Elements of Flow in LCC Upper and the Aqueduct

	Canal U/S Aqueduct	Aqueduct D/S end.	Canal D/S Aqueduct
CHANNEL DATA			
Bed width (ft.)	210	110	240
Side slope	2 : 1	Vertical	2 : 1
Bed width flaring		1 in 3.6	1 in 4
CURVE DATA			
Deflection angle	$\simeq 45°$		$\simeq 85°$
Radius (ft.)	5,000		1,150
Radius : Bed width	$23.8 = \frac{1}{0.038}$		$4.8 = \frac{1}{0.208}$
HYDRAULIC DATA Q=8,000 cusecs.			
Depth of flow (ft.)	10.3	9.2	10.0
Average velocity (ft./sec.)	3.18	7.90	3.08
Froude Number	0.18	0.46	0.18
Depth : Radius	0.002	—	0.009
HYDRAULIC DATA Q=12,000 cusecs			
Depth of flow (ft.)	12.9	11.4	12.78
Average velocity (ft./sec.)	3.95	9.58	3.54
Froude Number	0.20	0.50	0.18
Depth : Radius	0.003	—	0.011

4. MODEL STUDY

The phenomenon of open channel flow in bends, involving separation possibilities depends on the interaction of gravitational, viscous, pressure and inertia forces, provided the model scale is not too small to involve surface tension. The gravitational force is important because it is a free surface phenomenon and changes of surface elevation like depth of flow, superelevation, waves etc., are dependent on it. The viscous forces are important in determining the rate of growth and decay of secondary flow and hence their effect on the velocity profiles of the flow. The inception of separation is a boundary layer phenomenon, which depends on the Reynold's number of the boundary layer and the pressure gradient. The interaction between the main flow and the zones of separation, in the shape of additional shear, turbulence generation and

dissipation and consequent loss of energy is however dependent on the viscous forces. As the model fluid is restricted to canal water supply, it is impossible to satisfy all the requirements of similarity, with a small scale model. The design of model, carried out for the study of proposed design of aqueduct and the following relocated channel will therefore be explained to show as to how the limitations of similitude can be visualised in such a case.

The first step is to determine the predominant force involved in the phenomenon. In this case it is obviously the gravitational force. The model has thus to be designed on the Froude's law of similarity. The model scale is restricted by the limitations of discharge and space available. The area available for the model dictated a horizontal scale of 1/30. From an analytical derivation of the strength of cross flow, developing in flow in bends, it is known (3.1) that

$$\frac{vr}{vo} \propto \frac{h}{r}$$

Where

vr : is the maximum radial velocity of cross flow in the vertical

vo : is the average longitudinal velocity on the central vertical (in the main flow),

h : is the depth of flow and

r : is the radius of the bend.

The helicoidal flow is an important feature of the flow in bends because it determines the flattening of the velocity profiles in the vertical and the velocity distribution across the channel. It is therefore necessary to maintain similar ratio of $\frac{h}{r}$ in the model and the prototype. The model should therefore be geometrically proportioned.

The Reynold's number of flow in the main channel is of the order of 10^7 and that in the aqueduct is of twice this magnitude. The prototype channel is brick lined. Taking the median protuberance of such a surface as 0.008, the roughness Reynold's number of the flow is about 160 *i.e.*, the flow is in fully rough turbulent regime. For a model proportioned to Froude's similarity law, the ratio of the model and prototype Reynold numbers is given by $Lr\ 3/2$ where Lr is the linear scale ratio. For the adopted scale of 1/30, the model flow Reynold number would be of the order of 10^5 and for a linearly reduced surface roughness, the roughness Reynold number on the model would be 1.6, which would place the model flow in smooth turbulent regime. It is understood that although the velocity profiles in both the model and prototype would remain logarithmic, but in the former case, the roughness would be a function of both the relative roughness and the Reynold's number of the flow and

will have to be accordingly determined. It would also be seen that due to a lower Reynold's number of the model flow the viscous force will be comparatively more dominant than in the prototype. The smoothest surface that could be economically provided in the model was a neat cement finish. The median roughness size for this would be 0.0003 which would be a linear reduction of the prototype roughness but due to the smaller Reynold's number in the model, it would generate higher friction and thus the value of Chezy's C in the model would be about 15 per cent lesser than in the prototype. Now it has been analytically shown (3.1) that in wide shallow bends.

$$\frac{x}{h} \simeq \frac{2.3\,C}{g} \qquad ..4.1$$

$$\theta\, lim \simeq \frac{1.5\,C}{\sqrt{g}} \cdot \frac{h}{r} \qquad ..4.2$$

and

$$\frac{1}{h} = \frac{C^2}{2g} \cdot ln \frac{k}{p} \qquad ..4.3$$

Where

x is the distant beyond the geometrical end of the curve in which circulation in term of radial velocity vr, decays to about 10 per cent of its maximum constant value in the bend

h is the average depth of the flow

C is the Chezy's coefficient

$\theta\, lim$ is the angle in radians from the physical beginning of the bend in which the circulation (vr) grows to its maximum value

l is the length of flow downstream of the curve, in which the maximum velocity distribution inequality in the section would reduce from k per cent to p per cent over the average

It would thus be known that the both x and θ lim would be about 15 per-cent and 1 about 23 per cent lesser on the model than on the prototype.

Since the model value of C is about 85 per cent of the prototype value it would require about 40 per cent more slope than the prototype. The prototype slope is small (1/11100) and for a prototype length of 5,000 feet would require a drop in the model bed level of about 0.015 feet, while for the required model slope, this drop would be 0.021 feet. A slope of this order in the bed level is difficult to control on the model. As such the bed slope was provided as an average between the Aqueduct and the Sagar Regulator allowing a drop of 0.02 feet.

For the possibilities of separation, the pressure gradient on the model would be similar to that of the prototype, because models based on Froude's criterion, also have similar Euler's number provided the Reynold's number are large enough. The growth of boundary layer and its conversion to turbulent

layer is however slower on the models. Thus assuming that the boundary layer has not become turbulent before the adverse pressure gradient becomes operative, it can be concluded that the inception of separation will take place earlier on the model than on the prototype. This would only tend to make the model slightly more sensitive to separation.

The model of LCC Complex was constructed at Nandipur Field Research Station to a geometrical scale of 1/30 representing LCC Upper from about 400 feet upstream of the Aqueduct to Sagar Regulator. The model was constructed in brick paving on excavated bed, and was provided with rich cement sand mortar lining. The surface was finished with neat cement finish. The discharge scale was determined from Froude's law. This required about 1.63 cusecs for 8,000 cusecs prototype discharge and 2.44 cusecs for 12,000 cusecs discharge. The water supply was obtained from the high level 75 cusecs channel and was measured on a 2.0 feet standard rectangular sharp crested weir with end contractions suppressed. The supply channel to the weir was also standard. A spill weir was provided upstream of the control gate to maintain steady discharges in the model. The supply approaching the model was baffled through screens filled with gravel. The channel curve in the reach upstream of the aqueduct was not represented.

The model was verified for prototype discharges of 5,000, 8,000 and 12,000 cusecs. In order to maintain uniform flow conditions two static tubes were installed on the left bank of the flow in the straight reach about 70 feet apart and aligned upstream. The differential reading on a water manometer was determined for uniform flow conditions which was maintained in subsequent testing. It was thus ensured that no heading up is created at Sagar Regulator in the model. In addition, straight edge rails were installed on both sides of the model channel along the Aqueduct and the curve and also at specific points in the straight reach downstream of the curve to facilitate observations of velocity profiles.

Lower Chenab Canal Upper, upstream of Sagar Regulator has a capacity of some 11,000 cusecs which is evenly distributed in Upper Gugera Branch and Lower Chenab Canal Lower. LCC feeder, with a capacity of 4,100 cusecs has been constructed from Q-B Link to feed the main offtakes of LCC Lower, so that in its future operation, LCC Lower may only draw 1,000 cusecs. With 7,000 cusecs as the capacity of Upper Gugera Branch, the new design capacity of LCC Upper would be 8,000 cusecs. For flexibility of operation in future, it was however proposed to leave LCC Lower untightened with its present capacity of 6,000 cusecs, and provide a maximum design capacity, in LCC Upper at Sagar of 12,000 cusecs. The future operation of LCC Upper at Sagar was thus envisaged as follows:

LCC Upper at Sagar	Upper Gugera Branch	LCC Lower
12,000 Cs.	7,000 Cs.	5,000 Cs.
8,000 Cs.	7,000 Cs.	1,000 Cs.
5,000 Cs.	4,000 Cs.	1,000 Cs.

This was accordingly assumed as the discharge distribution in the model study and the proposals were tested for each of these conditions.

5. MODEL BEHAVIOUR OF DESIGN CURVE

The original design layout of the relocated LCC Upper, as shown in Figures 3.2 and 3.3, was tested on the model for discharges of 5,000, 8,000 and 12,000 cusecs. It was noted that for all the three discharges, the flow separated from the banks over most of the 1,150 feet radius curve. The extent of surface rollers, which indicated zones of separation, was marked for each of these discharges. This is shown in Figures 5.1 and 5.2. Reference to these figures will show that for 12,000 cusecs the rollers extended on the outer bank to a maximum of 90 feet width, over a length of about 900 feet. A small roller also formed on the inner bank, just downstream of the Aqueduct. The flow concentrated on the inner bank for about one-third of the deflection angle and then switched over to the right bank. In this reach a roller of maximum width of 105 feet and some 800 feet length formed on the inner bank. The extent of rollers was also substantial though smaller for the lower discharges. No sand was fed in the model, but at the conclusion of each test, the small quantity of sand carried by the model water supply was found deposited at the location of the rollers.

The velocity profiles were observed in the Aqueduct, the curve and the straight reach upstream of Sagar Regulator. The profiles for the Aqueduct were used for checking if the flow entering the model was symmetrical. This was found to be so. On the prototype, the Aqueduct is preceded by a 5,000 feet radius, 45° curve which ends, about 300 feet upstream of the Aqueduct. This curve would take about 450 feet of length of flow to reduce the cross flow velocity to almost nil. Also the normalisation of velocity distribution in the cross section would take about 5,000 feet downstream of the physical end of the curve. The Aqueduct would thus have been susceptible to asymmetrical velocity distribution. This is however obviated by the 50 per cent contraction at the Aqueduct which should make the velocity distribution across the section uniform. It is for this reason that the upper curve was not represented on the model and the Aqueduct was checked for uniform distribution across the section.

Data on the velocity profiles, observed in the curve and the straight

FIG 51

LCC - COMPLEX

RELOCATED LCC UPPER

Model Performance of Original Design

Separation Zones

for

Q = 12000 Cs.

Scale - 1 CM = 100 ft.

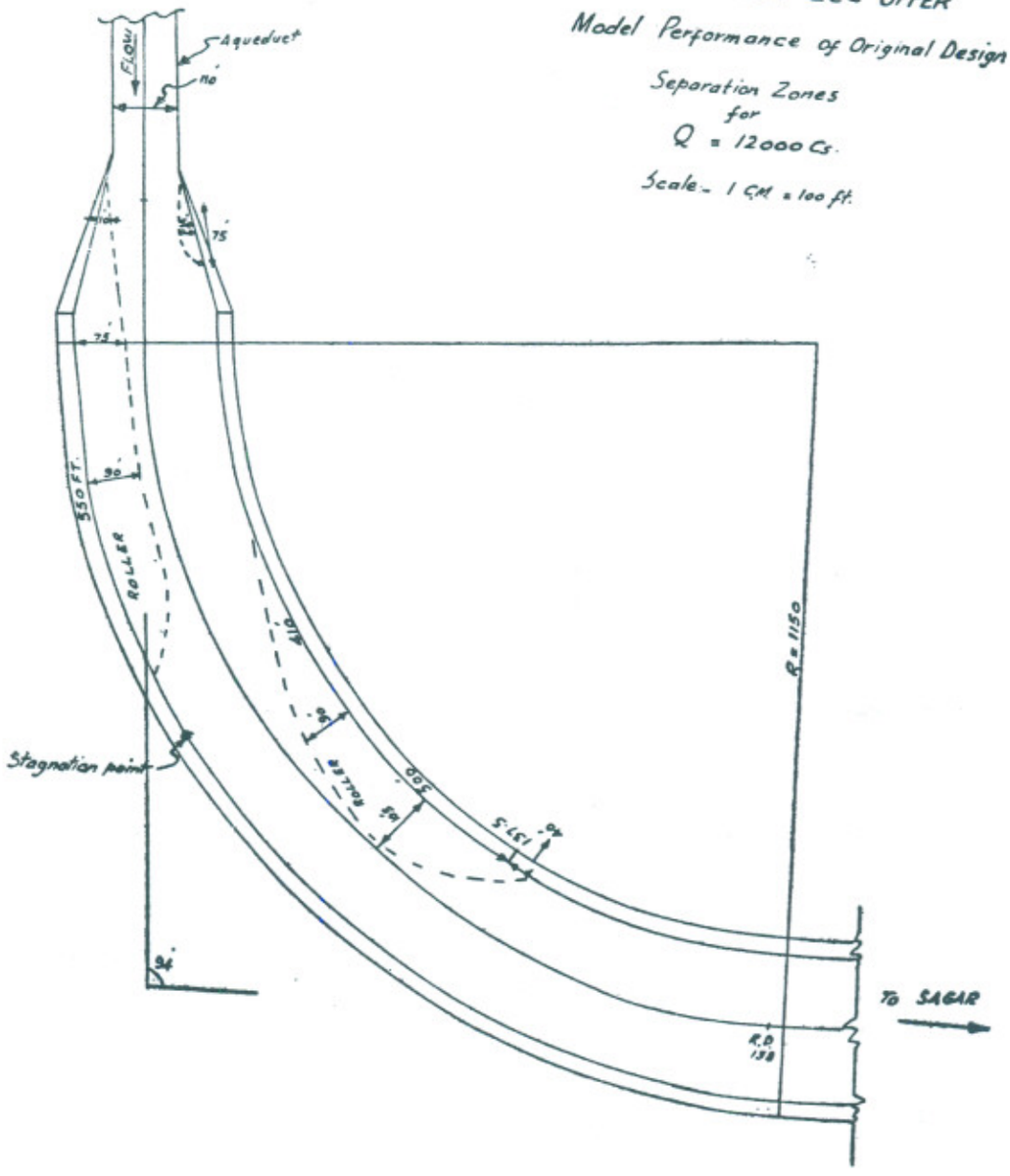

FIG 52

LCC - COMPLEX

RELOCATED LCC UPPER

Model Performance of Original Design

Separation Zones

for

Q = 12000 CS

Scale: 2 CM = 100 ft.

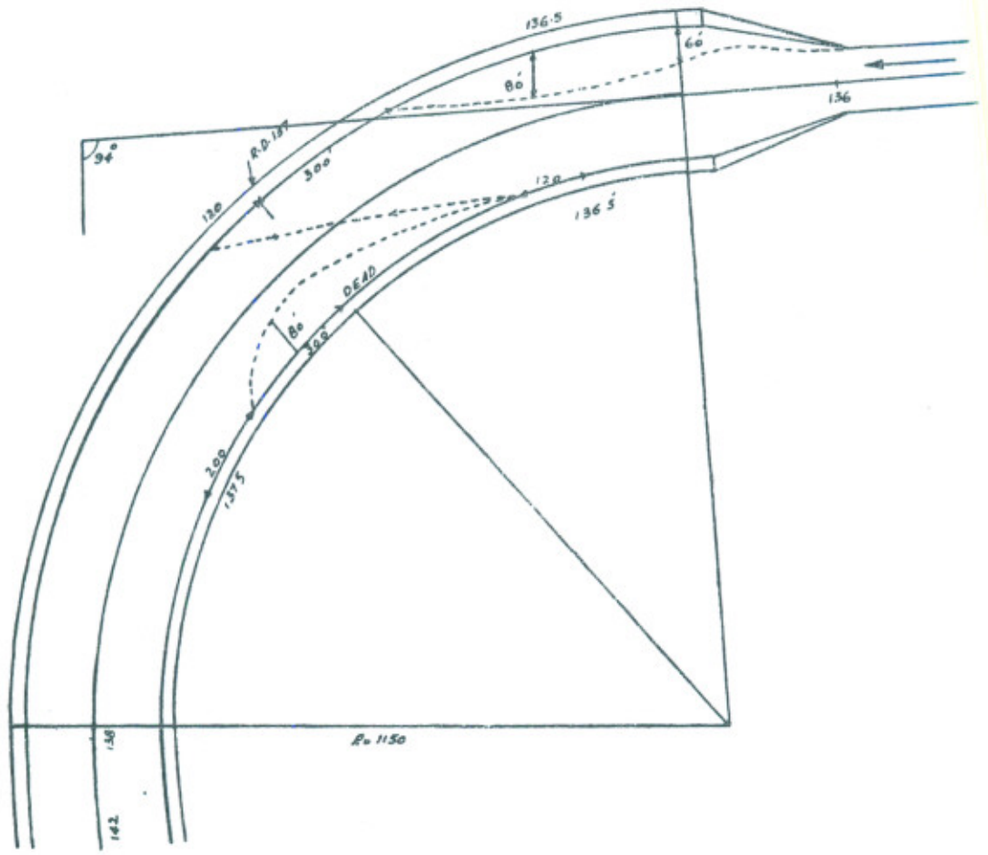

reach, have been analysed by taking the average on each vertical and then averaging these averages over the bed width. The normalised average velocity ratio diagrams for each R. D. and for discharges of 12,000 and 8,000 cusecs are shown in Figure 5.3. The diagrams are such that area under each diagram is equal to unity. This makes the comparison between different proposals and discharges easy. The data presented in these figures would show that for the proposed design the normalised average velocity ratio varies from 0 to 2.0 in the curve. At R. D. 140 the velocity distribution varies from 0.7 to 1.5 for 12,000 cusecs and 0.85 to 1.3 for 8,000 cusecs.

Although the model study indicated that near Sagar Regulator at R.D. 141 a sufficiently uniform velocity distribution is attained in the section of the flow, the separation zones in the main curve were a disconcerting feature. It was considered that these had to be obviated for the following reasons:

(*i*) The losses caused due to separation would reduce the ultimate capacity of the canal. This was important, because in the original design a flatter slope had to be given downstream of the Aqueduct to cater for the additional length generated by the relocation.

(*ii*) The flow turns from the left bank to the right bank and is deflected therefrom. This could cause local damage to the brick lining by the excessive pressure thus generated.

(*iii*) There would be a tendency for the sediment in the main flow to concentrate in the separation zones. Due to the local inadequacy to transport sediment, shoal growth would thus take place. The outline of these shoals would vary with the channel discharge and thus an unsteady sediment discharge would be passed down the canal in waves of higher silt charge, whenever the discharge was varied.

(*iv*) It would be unaesthetic to have separation of such a large magnitude in the channel.

On account of these factors, it was decided to change the design, so as to eliminate the separation of flow in the curve.

Another feature noted on the model flow was the surface waves generated in the Aqueduct at discharge of 8,000 cusecs, which became much worse for 12,000 cusecs. Two canal road bridge piers had been provided on each end of the Aqueduct and these generated additional waves which reflected from the Aqueduct walls. As the flow emerged from the Aqueduct the surface waviness travelled a long away along the curve. It was obvious that the surface waviness was a result of high Froude Number in the Aqueduct (0.46 at 8,000 and 0.50 at

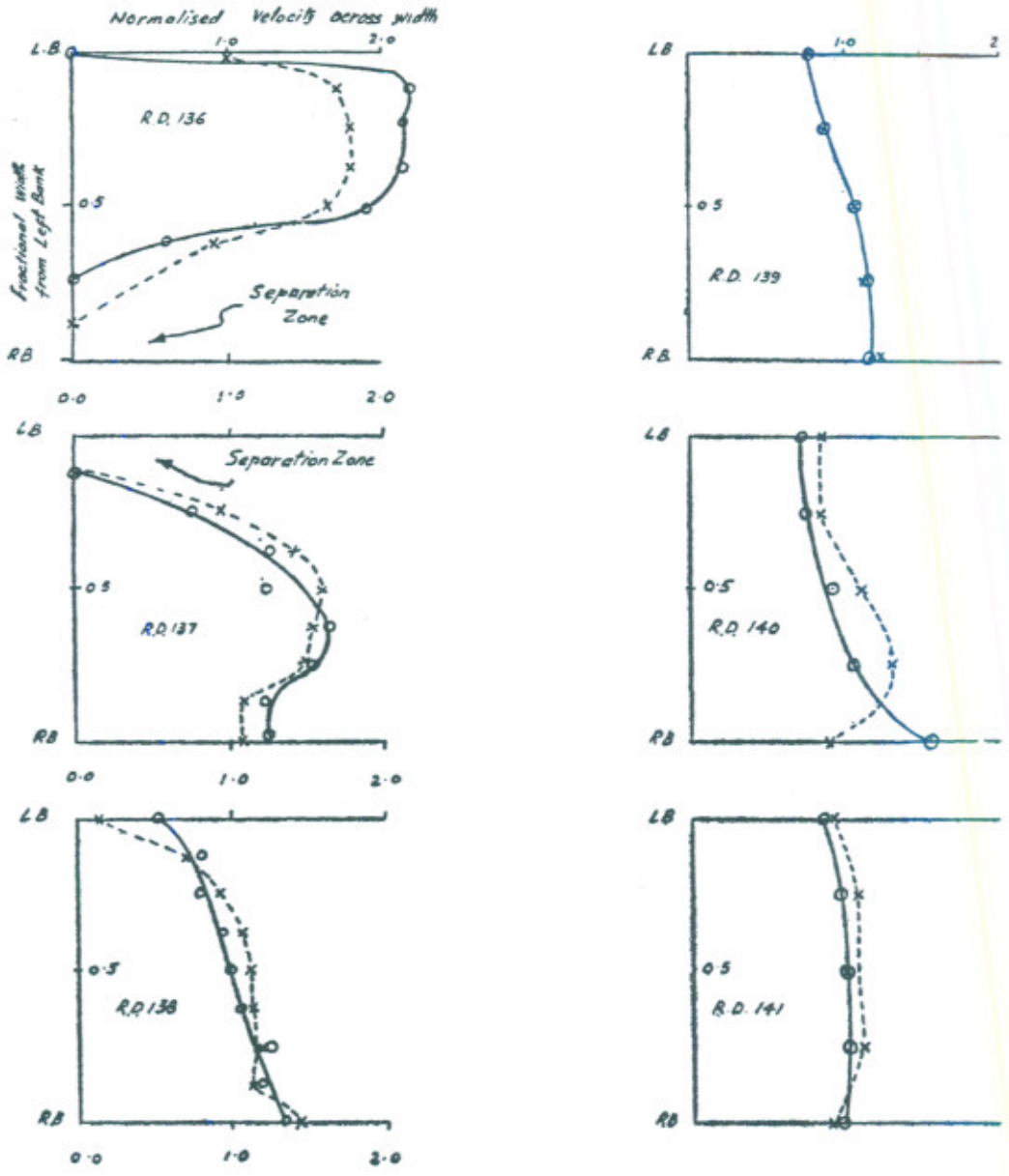

INDEX

Discharge 12000 Cs —o—

Discharge 8000 Cs --x---

Note: In these diagrams abscissa is average vel in each vertical divided by avg velocity is section.

Ordinate is fractional distance from Left Bed Line

FIG: 5.2

LCC COMPLEX

MODEL PERFORMANCE OF ORIGINAL DESIGN Circular Curve Radious 1150

NORMALISED VELOCITY DISTRIBUTION IN SECTION

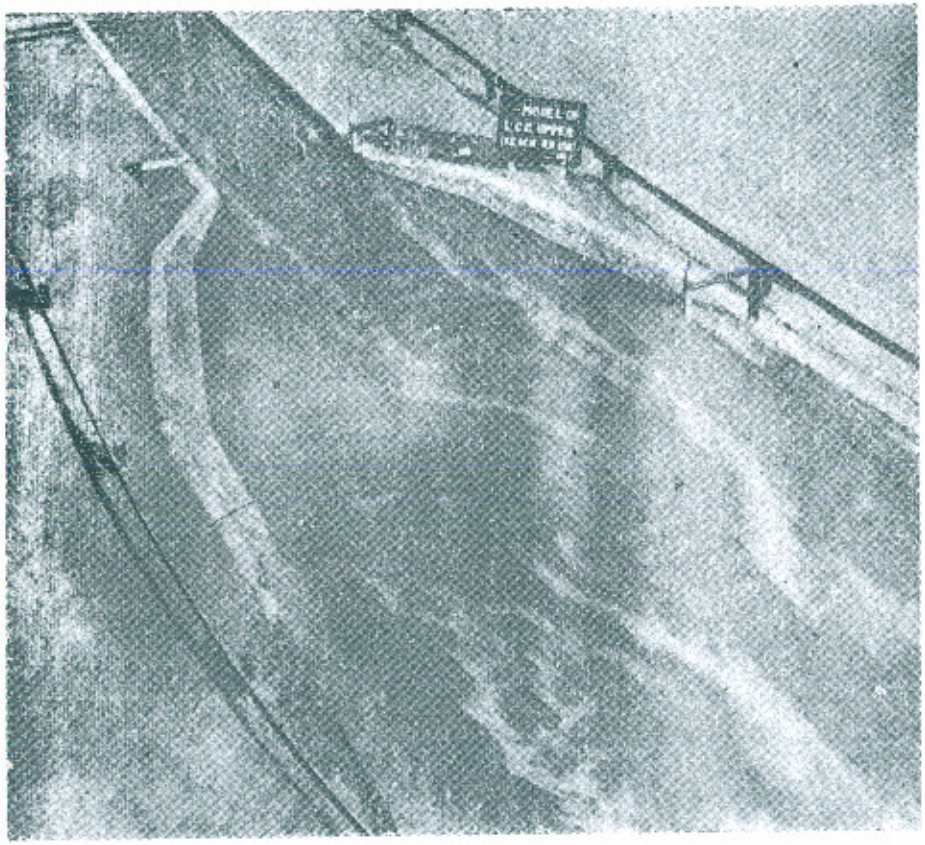

Q=12,000 Cusecs

Fig. No. 5.4 (*a*)
LCC COMPLEX
Relocated L.C.C. Upper Original Expansion
Aqueduct Straight Outfall

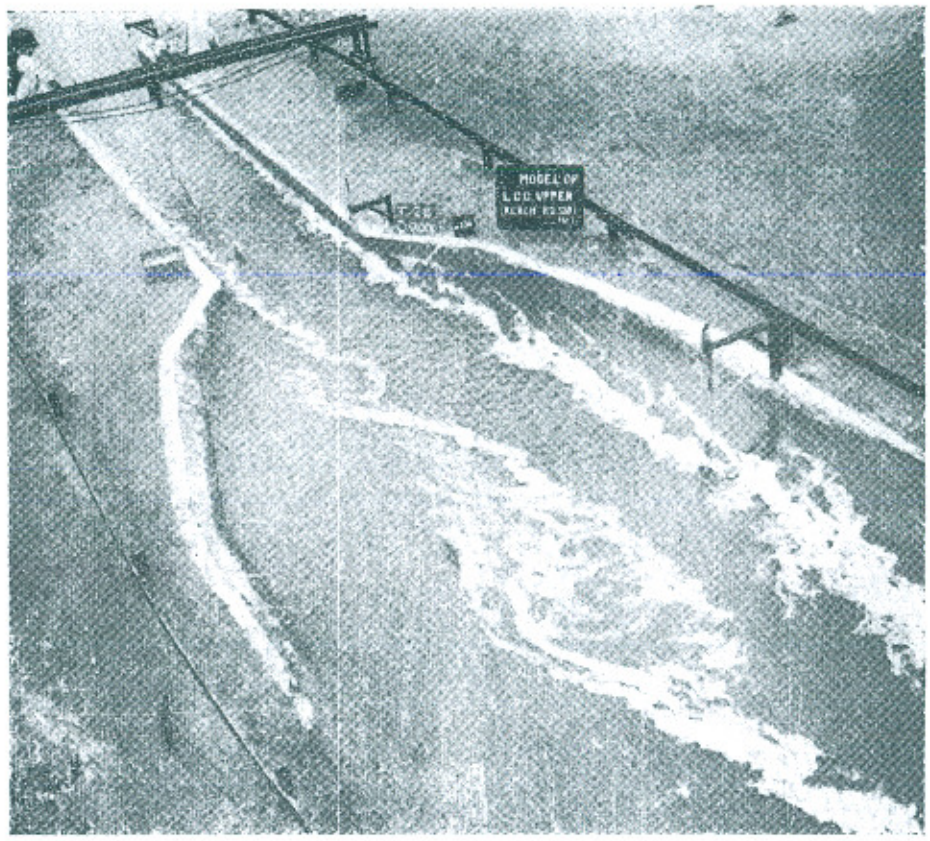

Q=8,000 Cusecs

Fig. No. 5.4 (*b*)
LCC COMPLEX
Relocated L.C.C. Upper Original Expansion
Aqueduct Straight Outfall

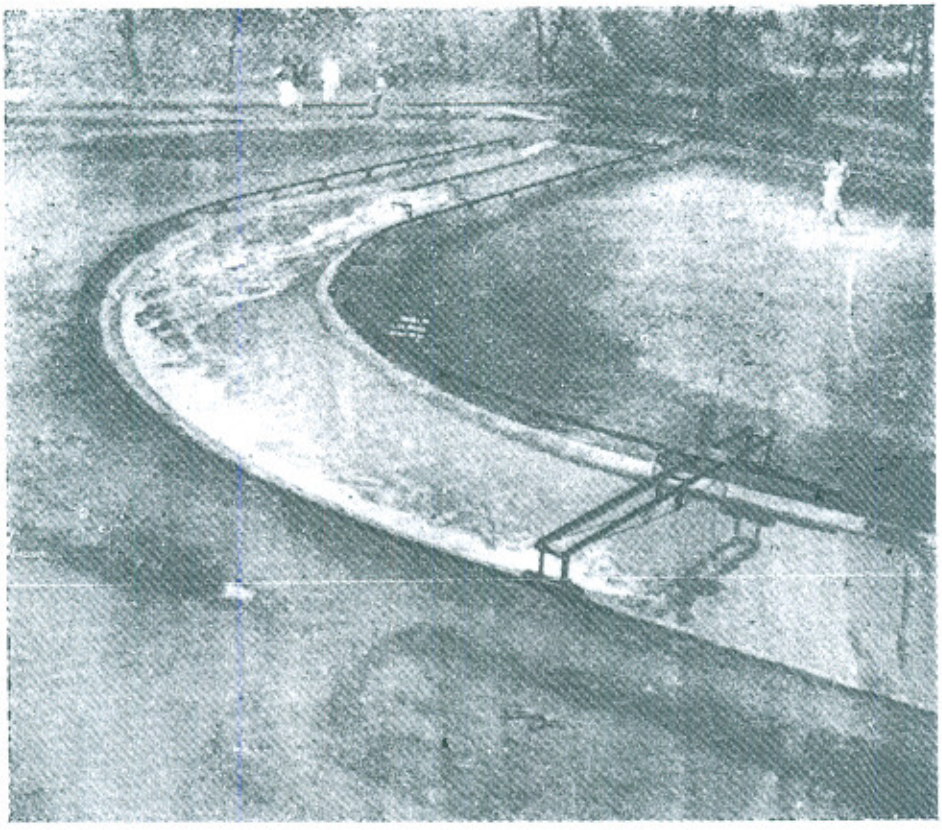

Q = 12,000 Cusecs

Fig. No. 5.5 (*a*)
LCC COMPLEX
Relocated L.C.C. Upper Original Design
Flow Pattern with 12,000 Cs. Discharge

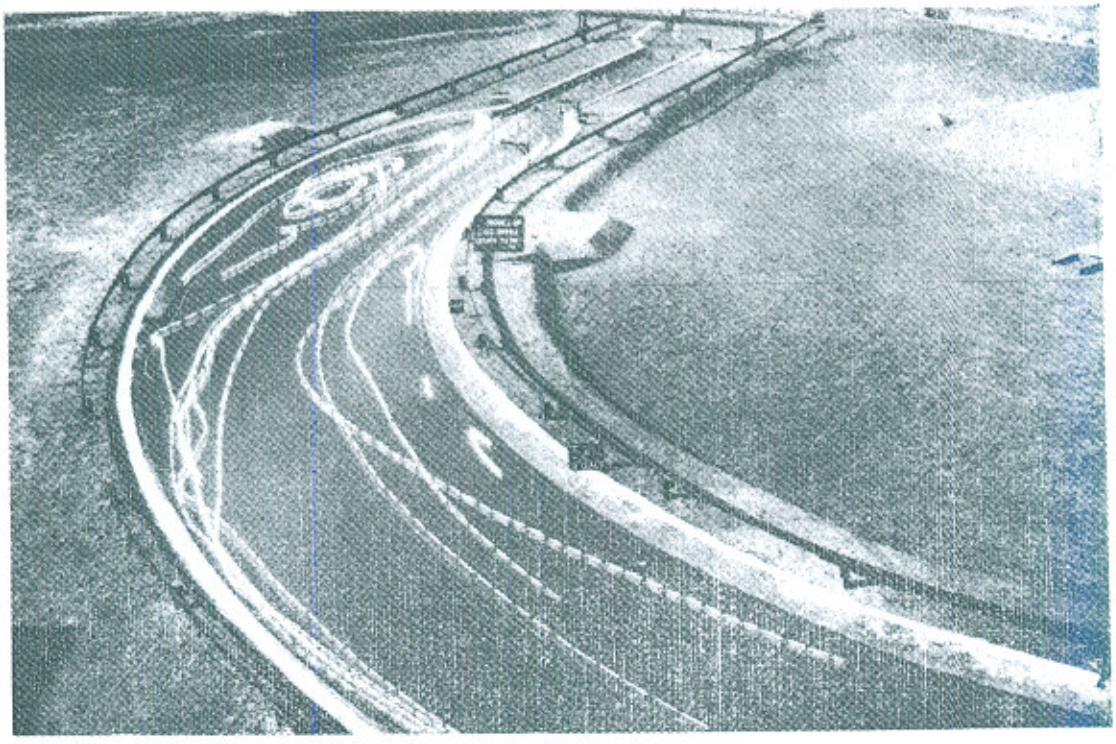

Q = 8,000 Cusecs

Fig. No. 5.5 (*b*)
LCC COMPLEX
Relocated L.C.C. Upper Original Design
Flow Pattern with 8,000 Cs. Discharge

12,000 cusecs). The only way to reduce these surface disturbances was to reduce the contraction at the Aqueduct and eliminate the bridge piers. It was however learnt that both these features could not be changed and as such were taken as unalterable in the design modification.

As a first step, the curve downstream of the Aqueduct was eliminated and a temporary straight outfall was provided to check the contribution of the downstream expansion transition of the Aqueduct in the separation suffered in the curve. A discharge of 12,000 cusecs was run and it was found that the jet issuing from the Aqueduct did separate from the boundaries just downstream of the end of the crossing. The expansion was found to be so inadequate, that the jet oscillated between left and right sides periodically. The flow pattern for this condition is shown in Figures 5.4 (*a* and *b*). The distance between the end of the Aqueduct and the beginning of the curve is only 259 feet. It was therefore not considered possible to provide an entirely separation free expansion transition. The flow pattern through the Aqueduct and the curve for a discharge of 12,000 and 8,000 cusecs is photographically shown in Figures 5.5 (*a* and *b*).

A number of devices, like compound curves (of shorter radius followed by flatter ones) and splitter vanes were tried on the model. It was found that even when the downstream transition had been changed to an elliptical one with 600 feet length or double cubic curves, the separation zones could not be eliminated. With vanes, the main disadvantage seemed that although they could be aligned for a given discharge to obviate separation from the channel boundary, it continued to persist on the vanes themselves and vertical vortices were generated at their ends. The separation at the vanes and the vortices at their ends became much worse for the discharges other than those for which they were aligned. It was apparent that as the streamline curvature and discharge distribution in the initial parts of the curve varied with discharge, fixed vanes could not solve the problem.

6. OPEN CHANNEL FLOW IN CURVES

When uniform flow in a straight prismatic channel, approaches a curve in plan, it undergoes certain changes in the velocity distribution and pattern, which extend both to the reach upstream (to some extent) and downstream (for a considerable length) of the bend. Within the curve itself the free surface on the outer bank rises, a helicoidal flow is super-imposed on the bend and flow at certain locations tends to separate from the solid boundaries. The knowledge of these characteristics is important in the context of present problem. They will be therefore, discussed briefly.

Flow in initial part of the bend : Just before the physical beginning of the bend, the concentration (and velocities) along the inner bank increase. In the initial part of the bend, the concentration increases still further, so that the maximum velocity isovel is near the inner bank and the minimum velocity isovel near the outer bank. As the flow progresses along, the maximum velocity isovel moves from the inner to the outer bank (if the bend is large enough), and remains there. At the physical end of the bend, the flow undergoes another transformation, which tends to shift the maximum isovel still closer to the outer bank. This asymmetric velocity distribution across the width continues for some length in the straight reach till the normal distribution of straight reaches in achieved. In plan, the curvature of various stream lines is such that, near the beginning of the curve, the curvature is more than that of the channel and near the end it is lesser. Only in the central reaches of the bend, the curvature coincides with that of the channel.

Superelevation of Free surface : As the flow enters the bend, the free surface along the outer bank is raised by an amount which is very nearly given by $\frac{V^2}{gR}B$, where V is the average velocity of flow, B is the width of the channel, R is the radius of curvature and 'g' is the gravitational acceleration. This superelevation persists throughout the physical boundaries of the bend and abruptly vanishes at its end. The readjustment of velocities at the beginning (higher concentrations on the inner bank) and at the end of the curve (still higher concentrations on the outer bank) are a consequence of the creation and vanishing of the superelevation. It can, also be analytically shown, that if the flow approaching the curve has a uniform distribution across the width, the superelevation would cause the flow in the beginning of the bend to be a free vortex.

Helicoidal Flow : As the streamlines undergo a curvature in the straight reach immediately upstream and at the beginning of the bend an unbalanced force is created on the flow section due to non-uniform velocity distribution in the profiles. This force is such that a circulation is developed in the flow, the direction of which is of a right handed screw for a left handed bend and *vice versa.* The surface flow in this circulation is towards the outer bank and the bottom flow towards the inner bank. For reasons of continuity downward flow would develop on the outer bank and an upward flow on the inner bank. The effect of the banks is however felt in a width of about one to two times the depth on each bank. In the central portion of the section the circulation is independent of the channel width. It may be noted that this circulation is entirely caused by the non-uniformity of the velocity profiles and if the profiles were uniform (as in uniform flow of ideal fluid), the

circulation would not develop.

The strength of this circulation, increases along the bend, till it reaches a maximum value (in terms of the radial velocities), after which it continues with the same magnitude. After the physical end of the channel curve, the circulation is dissipated in the straight reach downstream.

As the velocity profiles are such that the velocity is maximum near the surface and reduces towards the bed, the longitudinal momentum of the flow on the outer bank increases, while that on the inner bank decreases. This is the cause of readjustment of flow within the bend from a free vortex initially generated. Also as the result of the circulation, the velocity profiles becomes "fuller", that is the velocity nearer the bed increases.

Separation : At the beginning of the bend, the imposition of super-elevation (and reduction of velocity) causes an adverse pressure gradient on the outer bank. Similarly at or near the end of free vortex flow where the maximum isovel leaves the inner bank, adverse pressure gradient is created again. If the curve is sufficiently sharp, separation of flow will be experienced at these locations. The tendency of separation would increase with increasing depth : width ratio and with flatter side slopes.

Although most of the characteristics of sub-critical open channel flow can be quantitatively predicted from approximate theories, the phenomenon of separation cannot be so predicted. This is because of the difficulty in predicting inception of separation in turbulent boundary layers, which is made much more complicated in this case by the presence of free surface. As extreme cases rectangular channels with centre line curvatures as large as the bed width have been tried with small depth : bed width ratio, without experiencing any separation. The qualitative conclusions about the effect of side slope and depth width ratio however hold and have a physical explanation. For flatter slopes, the momentum of the flow in the slope portion of the cross section is very small and hence its resistance to overcome adverse pressure gradient is also small. For flow in curves, the separation has to be tested on models unless conservative radius : bed width ratios are adopted.

From the above discussion, it will be seen that the actual curvature of stream lines in a circular bend is such that it is sharper in the beginning of the curve and flatter in the lower portion. This characteristic is also apparent in the stream lines resulting form a vortex-source combination of ideal fluid. Similar streamlines are also adopted for the diffuser vanes of centrifugal pumps. Also it is a fundamental approach in hydro- and aerodynamics to shape the solid boundaries according to the streamlines derived from potential flow analysis for ideal fluid. This is the case for aerofoil sections in aerodynamics and pier shapes and hydrofoils in hydrodynamics. Although in the case of flow in open

channel bends, there are characteristics of helicoidal flow, which alter the whole of the potential flow velocity pattern, it was decided to try the vortex-source streamlines as the boundaries of the transition curve. It was anticipated that the original design was such as to cause an adverse pressure gradient of the order of 10^{-2} due to surface elevation change and velocity reduction, for a discharge of 12,000 cusecs. The same gradient for an equiangular spiral would be of the order of 10^{-3} at the beginning and 10^{-4} at the end and thus the chances of separation would be reduced.

7. EQUIANGULAR SPIRAL AS IDEAL FLUID STREAMLINE

In the two dimensional flow of ideal fluid, the combination of a source and a vortex, would generate streamlines which are equiangular spirals. The derivation of the streamline function is given in almost all the standard text books (7.1) and will not be reproduced here in detail.

For a source of strength Q ($2\pi q$), the stream function in polar coordinates is

$$\psi_1 = -\left(\frac{Q}{2\pi}\right).\theta \qquad ..7.1$$

For a vortex of circulation $\Gamma(2\pi\mu)$, the stream function is $\psi_2 = +\frac{\Gamma}{2\pi} ln\ r$, where r, θ are the polar coordinates of any point in the flow field.

FIG. 7.1 Equiangular spiral streamlines for source - vortex combination

The arbitrary values of ψ_1 and ψ_2 are selected such that $\psi_1=0$ where $\theta=0$ and $\psi_2=0$ when $r=1$. ψ_1 and ψ_2 being scalar quantities, the stream function for a combination of a source and vortex with a common polar origin and similar boundary conditions is given by

$$\psi_c = \psi_1 + \psi_2 = -\frac{Q}{2\pi}.\theta + \frac{\Gamma}{2\pi} ln\ r \qquad ..7.3$$

Equation 7.3 can be rearranged as

$$r=ae^{m\theta} \qquad ..7.4$$

Where

$$a=e^{\Psi c/\mu} \quad \text{and} \quad m=\frac{q}{\mu}.$$

A set of these streamlines is shown in Fig 7.1. The streamlines depict a two-dimensional constant flow, which is turning and expanding at the same time, under a constant circulation. Also from the value of

$$m=\frac{q}{\mu} \text{ one may write } \frac{q}{\mu}=m=\frac{v_r.r}{v_\theta.r}=\frac{v_r}{v_\theta}$$

Where

v_r is the radial component and
v_θ the tangential component of velocity.

The resultant velocity vector v_s is given by

$$v_s=\sqrt{v_r^2+v\theta^2}$$

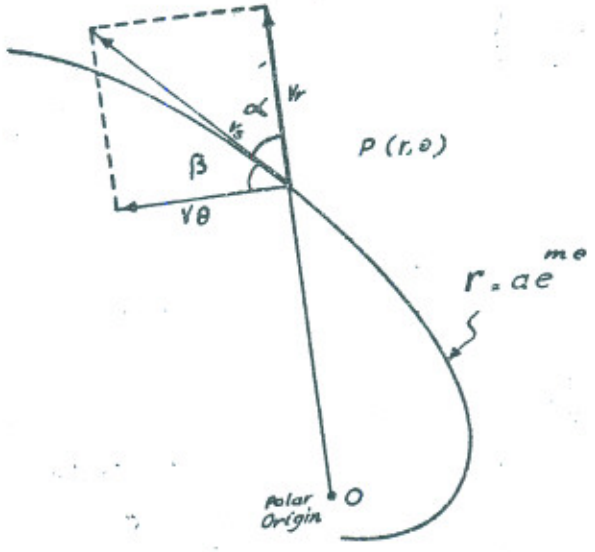

Fig: 7.2 Velocity Vector diagram in a Source-Sink Flow Field

Angles α and β (Fig 7.2) are complementary angles, and

$$\frac{v_r}{v'\theta'}=\tan\beta=\cot\alpha$$

since $\frac{q}{\mu}=m$ is constant for the flow field, α and β are the same for any point in the field, *i.e.*, the velocity vector diagram is represented by similar triangles. It may be noted that the smaller the strength (Γ) of the vortex the smaller is the value of angle α.

8. PROPERTIES OF EQUIANGULAR SPIRAL

The family of curves represented by equation 7.4 and shown in figure 7.1 are called equiangular spirals. For these curves the angle between the radius vector and the tangent to the curve (angle α in figure 7.2) is a constant. This can also be shown from the basic equation of differential calculus.

In polar coordinate, the angle ϕ between the radius vector and the tangent to the curve is given by

$$\tan \phi = r\frac{d\theta}{dr}$$

For equation 7.4

$$\tan \phi = \frac{r}{mr} = \frac{1}{m} = \text{constant}$$

A particular corollary of this property is that for a given equiangular spiral, the polar origin can be graphically determined.

The length of a curve in polar coordinates is given by

$$\frac{ds}{d\theta} = \sqrt{r^2 + \left(\frac{dr}{d\theta}\right)^2}$$

Where $\frac{ds}{d\theta}$ is the first derivative of length S with respect to the polar angle θ.

For equation 7.4

$$\frac{ds}{d\theta} = r\sqrt{1+m^2} = \frac{r}{\sin \alpha} \text{ and}$$

integration between two points $r, \theta \mid 1$ and 2 would yield

$$S_{1-2} = \left(\frac{r_2 - r_1}{\cos \alpha}\right) \qquad ..8.1$$

i.e., the length of the spiral between any two points is the quotient of the difference of the lengths of their radius vectors and cos α.

The radius of curvature for any curve is given by

$$\rho = \frac{(r^2 + r_1^2)}{r^2 + 2r_1^2 - rr_2} \text{ where}$$

$$r_1 = \frac{dr}{d\theta} \text{ and } r_2 = \frac{d^2r}{d\theta^2}$$

For equation 7.4

$$\rho = r\sqrt{1+m^2} = \frac{r}{\sin \alpha} \qquad ..8.2$$

which is also the length of its sub-normal. Thus the radius of curvature for any point on an equiangular spiral is proportional to its radius vector and can also be graphically determined.

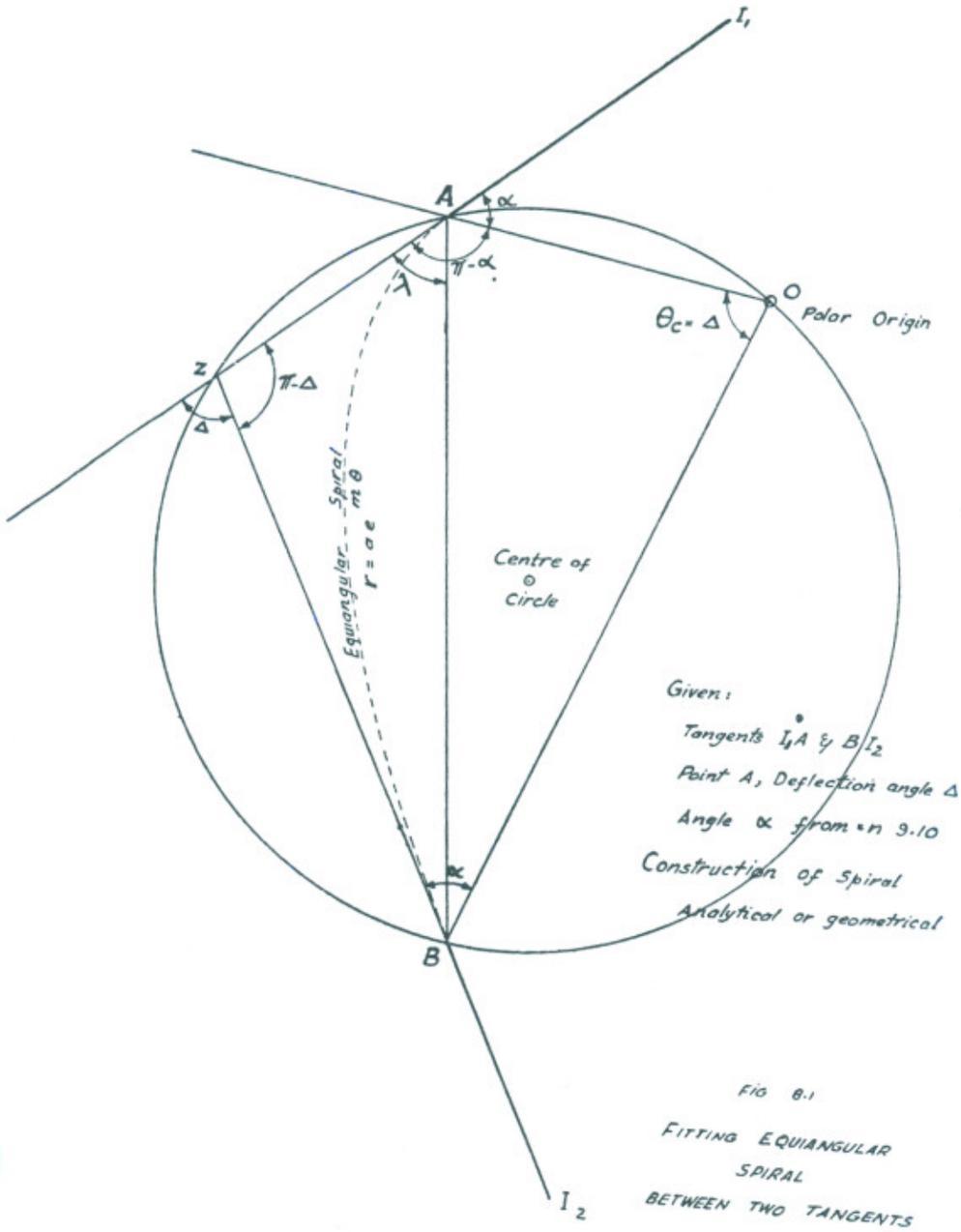

FIG 8.1

FITTING EQUIANGULAR SPIRAL BETWEEN TWO TANGENTS

Figure 8.1 shows two straight lines $\overline{I_1AZ}$ and $\overline{ZBI_2}$ with a deflection angle Δ. If an equiangular spiral is to be fitted between points A and B, such that it will be tangential to both I A and B I_2 then it can be shown (from the summation of the internal angles of quadrilateral OAZB) that the polar origin of the spiral must lie on the circle passing through points A, Z and B. Since from the geometrical theorem, one and only one circle can pass through three coplanar points, not in a straight line, this circle, on which the polar origin 0 lies is also unique. Also as the number of points possible on arc AOB is infinite, the number of spirals that will satisfy the condition of tangentiality at A and B is also infinite.

9. DESIGN OF EQUIANGULAR SPIRAL AS TRANSITION CURVE DOWNSTREAM OF AQUEDUCT

In order to design the equiangular spiral transition between the Aqueduct and the Lower Chenab Canal downstream, it is necessary to determine the equation of three spirals which would respectively represent the inner edge, the centre line and the outer edge of the bed width. Say these equations are:

$$\text{Inner edge } r_1 = a_1 e^{m\theta} \qquad ..9.1$$

$$\text{Centre line } r_0 = a_0 e^{m\theta} \qquad ..9.2$$

$$\text{Outer edge } r_2 = a_2 e^{m\theta} \qquad ..9.3$$

There are two requirements to be met with by this family of spirals. Firstly they should be tangential at their beginning and ends to the respective channels bed alignments and secondly, the normal channel bed width should increase from the downstream of the aqueduct (110 feet) to that on the main channel (240 feet). Also the starting point of the Centre line spiral (A) may be fixed. The end point of this spiral (B) shall however be determined from the fulfilment of these two conditions.

Now consider any two spirals say those of equations 9.1 and 9.2. Their equations for the two extreme radius vectors (at the beginning and the end of the transition) can be written as

$$r_{1a} = a_1 \qquad ..9.4$$

$$r_{0a} = a_0 \qquad ..9.5$$

$$r_{1c} = a_1 e^{m\theta_c} \qquad ..9.6$$

$$r_{0c} = a_0 e^{m\theta_c} \qquad ..9.7$$

Where subscripts a and c denote the conditions at the aqueduct and the canal ends of the transition and θ_c is the polar angle between the extreme radius vectors. The polar axis is assumed to be aligned along the radius vector at the beginning of the transition.

Since the angle between the radius vector and the tangent to the spiral is constant (Figure 7.2) equations 9.4 through 9.7 can be manipulated to yield.

$$(a_0 - a_1) = \frac{Ba}{\cos \alpha} \qquad ..9.8$$

$$(a_0 - a_1)e^{m\theta_c} = \frac{Bc}{\cos \alpha} \qquad ..9.9$$

Where B*a* and B*c* represent the half bed width of the aqueduct and the canal respectively.

Dividing equation 9.9 by equation 9.8 yields

$$e^{m\theta c} = \frac{Bc}{Ba} \qquad ..9.10$$

From figure 8.1, it is known that θc equals the deflection angle of tangents I_1A and BI_2 *i.e.*, angle Δ. This being a given value as is also the right hand side of equation 9.10 the value of m can be determined.

The next step is to determine the values of coefficients '*a*' in equations 9.1 to 9.3. Before this can be done, the location of point B on the tangent Z I_2 (figure 8.1) has to be determined for one of these equations (say equation 9.2)

In figure 8.1 let angle $ZAB = \lambda$ Then angle $OAB = \pi - \alpha - \lambda$ and angle $OBA = \alpha + \lambda - \Delta$. From the law of sines, in triangle OAB

$$\frac{OA = r_{oa}}{\sin OBA} = \frac{OB = r_{oc}}{\sin OAB} \qquad ..9.11$$

knowing m from equation 9.10 and $\theta c = \Delta$ and also that $\alpha = \cot^{-1} m$, equation 9.11 can be solved for λ. From figure 8.1 the equation of line *AB* (knowing its bearing and coordinates of point A) can thus be calculated. The location of point B is found by the intersection of lines AB and ZI_2. Having determined line AB equations of lines AO and BO can be found and hence the coordinates of polar orign O. The length of OA can thus be determined as the distance between points O and A and this equals the coefficient 'a_0' in equation 9.2. Once equation 9.2 is solved, values of a_1 and a_2 can be easily determined from equation 9.8. The layout of the spirals from the determined equations and coordinates of polar origin O can then be carried out.

As is evident from figure 8.1 the location of the point B and O as well as the values of coefficients '*a*' and the plotting of the spirals can be done geometrically once the value of exponent m (or angle α) and angle λ have been determined. In major field layouts, it will be however necessary to analytically determine the whole thing for reasons of accuracy of layout.

The method of fitting the equiangular spiral to the relocated LCC Upper downstream of the aqueduct will now be explained. The data of the two curves, the one preceding and the other succeeding the aqueduct are given in Table 9.1. The bearings of lines I_1I_2 and I_2T_2 are shown in Fig. 9.1. The cartesian origin in this figure has been placed at the grid coordinates as follows:

North 966000 Yards.
East 3591000 Yards.

The coordinates of points I_1, I_2 and T_2 are given in feet, with respect to the new origin as below, along cardinal axes North and East.

Point	Coordinates (feet)	
	N	E
I_1	6919.65	6047.82
I_2	5131.29	2055.06
T_2	598.92	3650.94

If the spiral begins at R. D. 136+000 the coordinates of point A (Fig 9.1) are calculated as below.

Point	N	E
A	5690.15	3305.00

From equation 9.10

$e^{m\theta} = \frac{120}{55} = 2.18182$, and

$\Delta = \theta = 1.4882326$ radians

$m = 0.524218 = \text{cotangent } \alpha$

$\alpha = 62° — 20' — 08.4''$

Introducing values of α and Δ in equation 9.11 and expanding, the value of λ is obtained as 48°—20′—57.5″ and bearing of line AB as S 72°—28′—37.5″ W. Equations of lines I_2T_2 and AB are as below

I_2T_2 : $Y = -2.840094X + 10967.85$

AB : $Y = 3.16317X - 4764.13$

Point B being at the intersection of these lines has coordinates

$Y = 3{,}525.20$

$X = 2{,}620.57$

TABLE 9.1

L C C COMPLEX

DATA OF CURVES ON RELOCATED

L C C UPPER

(PROPOSED DESIGN)

Station	Line	Coordinate (Yards)		Bearing	Distance Feet	Deflection Angle
		North	East			
POT_1		968984.44	3593273.00			
	POT_1-PI_1			S20°-46′-00″W	2177.55	
PI_1		968306.55	3593015.94			45°-06′-20″
	PI_1-PI_2			S65°-52′-20″W	4380.17	
PI_2		967710.43	3591685.02			85°-16′-10″
	PI_2-POT_2			S19°-23′-50″E	4810.82	
POT_2		966710.43	3592216.98			

Station	Line	Radius Feet	Length of Curve Feet	Length of Straight Reach Feet	R.D. 1000 Ft.	
					PC	PT
POT_1						131—000
	POT_1-PI_1			101.09		
PI_1		5000	3964.80		131+101.09	135—065.89
	PI_1-PI_2			1244.95		
PI_2		1150	1711.46		136+310.84	138+022.30
	PI_2-POT_2			3752.06		
POT_2					141+744.36	

Source: Drawing No. 1341 Job No. TK-H_1 Sheet . . . File No. L-979

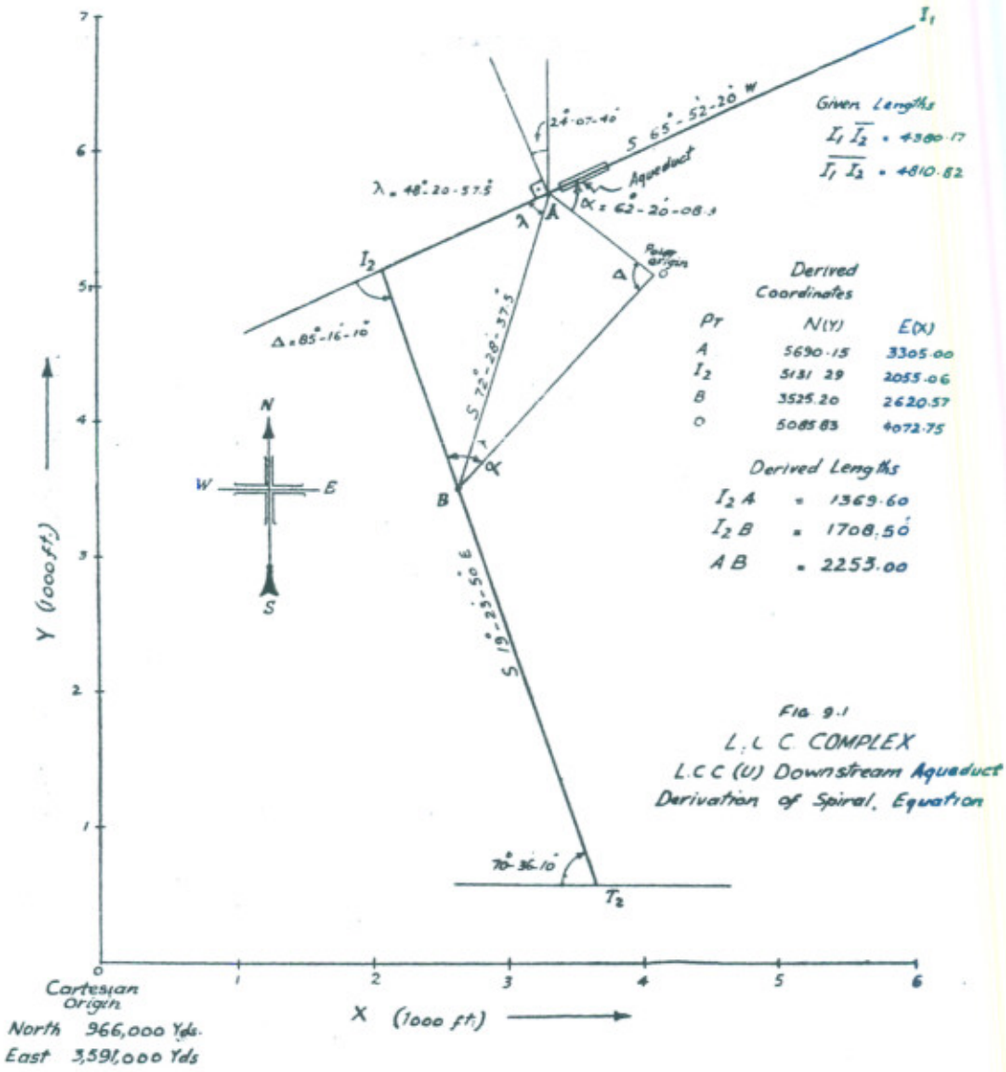

FIG. 9.1
L.L.C. COMPLEX
L.C.C. (U) Downstream Aqueduct
Derivation of Spiral Equation

The length of line BT_2 = 3102.40
And R. D. of Point B = 138+672.0
From bearings of radius vectors $\overline{OA}$ and $\overline{OB}$ their lengths are calculated as
OA = 977.06 feet = r_{o1}
OB = 2131.78 feet = r_{o2}

As a check $\frac{r_{o1}}{r_{o2}}$ = 2.181835 against 2.181818

The equation for the centre line spiral is therefore

$$r_o = 977.059\, e^{0.52422\,\theta}$$

Now $(a-a_o) = \frac{55'}{\sin \alpha}$ = 62.099 ft.

Therefore equations for inner and outer edges are defined as

$$\text{Inner edge} \quad r_1 = 914.960 \; e^{0.524220}$$

$$\text{Outer edge} \quad r_2 = 1039.158 \; e^{0.524220}$$

Where θ varies from 0 to 1.4882326 radians. Knowing the coordinates of point A the offsets for points on the inner and outer edge spirals are calculated on rays at 5° interval from radius vector OA, which is taken as the polar axis. The coordinates, thus calculated are given in Table 9.2.

Length of spiral is given by equation 8.1

Lc = 2487.76 Ft.

RD point B = 138+487.76 and New R. D. point T_2 = 141+590.12

The spiral causes a net saving of 184.24 feet in the length of curve between the Aqueduct and Sagar Regulator.

10. MODEL PERFORMANCE OF SPIRAL

The spiral, as calculated in Table 9.2 was laid out on the model between the Aqueduct and the straight reach of LCC Upper. The layout of the spiral is shown in Figure 10.1 in relation to the Aqueduct and Sagar Regulator. The model construction, scaling and operation was done as described in part 4.

Visual observation of the flow did not indicate any separation from the Aqueduct down to the regulator and the vortices noted with vanes were also absent. At discharge of 12,000 cusecs the wave generation in the Aqueduct, was noted, as in the original design. The flow approaching Sagar was also far more uniformly distributed in the section than with the circular curve or other layouts.

Detailed velocity observations were made in the spiral and at R. D. 140 at cross sections normal to centre line. The velocity data have been presented in Figure 10.5 in a normalised velocity ratio distribution curve, for discharges of 8,000 and 12,000 cusecs. It may be noted that throughout the spiral curve, the live stream fills the whole of the bed width. As is normal for the flow in curves the velocity on the outer bank increases over that on the inner bank. The velocity distribution at R.D. 140 (about 1,000 feet upstream of Sagar Regulator) is more uniform than evidenced with the circular curve (Figure 4.3). For a discharge of 5,000 cusecs, it was noted that the flow in the section remained symmetrical up to R.D. 137+500 but in reach R.D. 138 ± 500, the left bank velocities were too small to be measured. Although no reverse flow was evidenced, it was considered an undesirable feature. It was therefore decided to try a superelevation of the bed in the initial reaches of the spiral.

TABLE 9.2

L C C COMPLEX

L C C UPPER REACH

DOWNSTREAM AQUEDUCT

Coordinates of Points on Bed Lines of the Spiral Transition.

$$r = a\, e^{m\theta}$$

Point	X_o	Y_o	X_1	Y_1
	Inner edge		Outer edge	
1	3353.80	5650.75	3390.00	4449.17
2	3272.38	5610.39	3256.21	5728.57
3	3189.22	5559.74	3161.80	5682.60
4	3108.12	5499.43	3069.27	5624.07
5	3029.08	5429.14	2977.19	5555.57
6	2953.06	5348.51	2887.40	5475.73
7	2881.16	5257.71	2801.08	5384.28
8	2814.42	5156.36	2719.39	5281.04
9	2754.40	5044.57	2643.61	5165.93
10	2701.39	4922.50	2575.11	5038.97
11	2657.56	4790.39	2515.24	4900.33
12	2624.01	4648.62	2465.46	2750.28
13	2601.79	4497.71	2427.24	4589.27
14	2592.41	4338.32	2402.08	4417.88
15	2597.18	4171.24	2391.43	4236.85
16	2617.47	3997.45	2395.89	4047.10
17	2654.44	3818.07	2619.93	3849.72
18	2711.81	3636.97	2661.92	3645.98
19	2722.86	3624.39	2527.07	3440.30
20	2750.00	7810.22	2528.27	3426.01

NOTE:

(1) The coordinates are in feet and refer to origin at absolute coordinates in the grid (Drg. No. 1341 Job No. TK-H1. sheet)

North (Y) 966,000 Yds.

East (X) 3,591,000 Yds.

(2) +ve Y is along North and +ve X along East of the grid.

(3) The side slope of wall may change from vertical to 2: 1 in about 300 feet length beginning from the downstream end of aqueduct.

(4) The bed may have a superelevation of 1.25′ across the bed at RD 136, linearly diminishing to 0 at the end of the curve.

(5) The cross slope will be given by raising and depressing the outer and inner banks respectively by equal amounts.

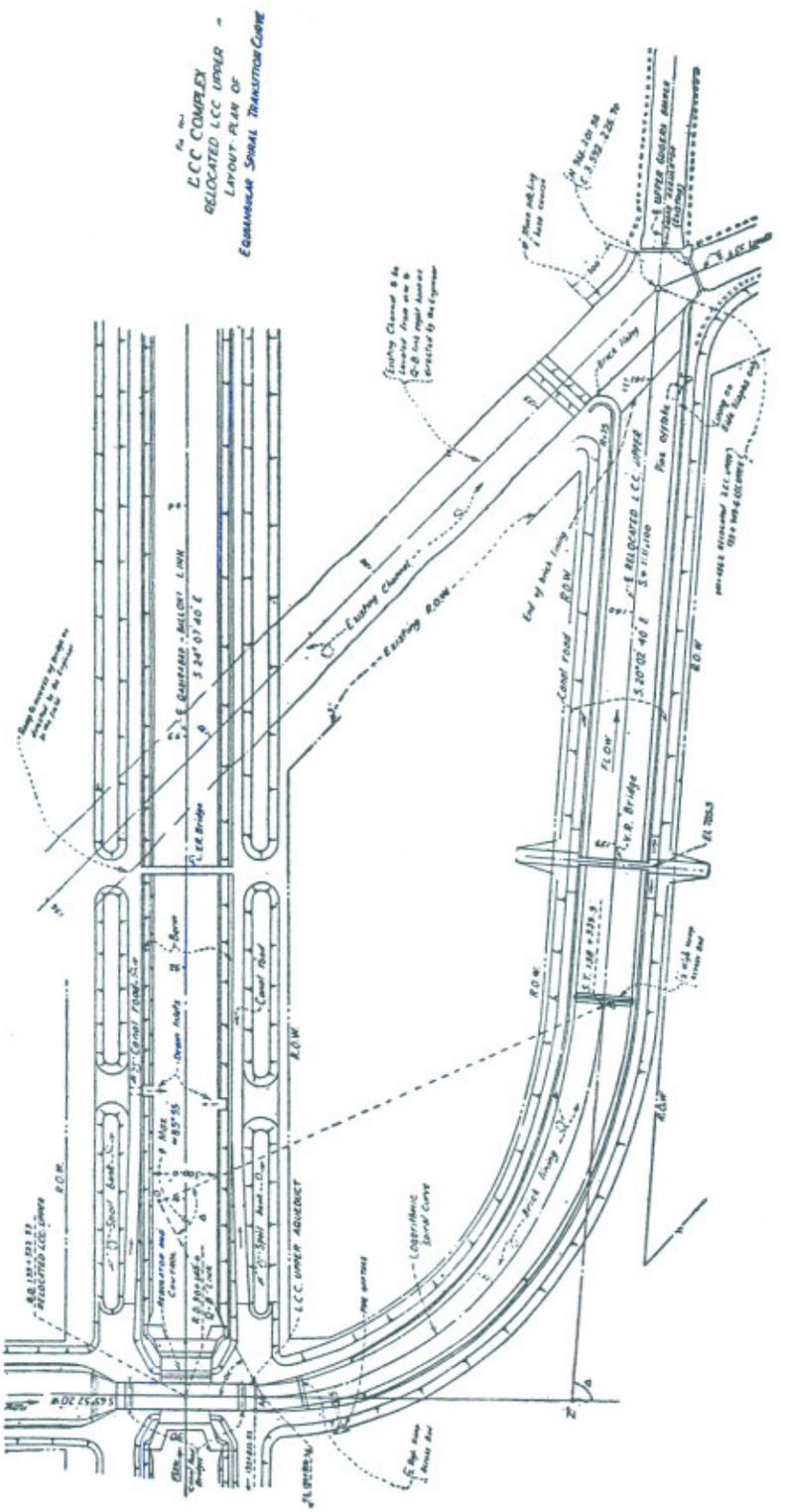
LCC COMPLEX
RELOCATED LCC UPPER -
LAYOUT PLAN OF
EQUIANGULAR SPIRAL TRANSITION CURVE
Existing Channel
Existing R.O.W.
LCC UPPER AQUEDUCT
Canal Road
R.O.W.

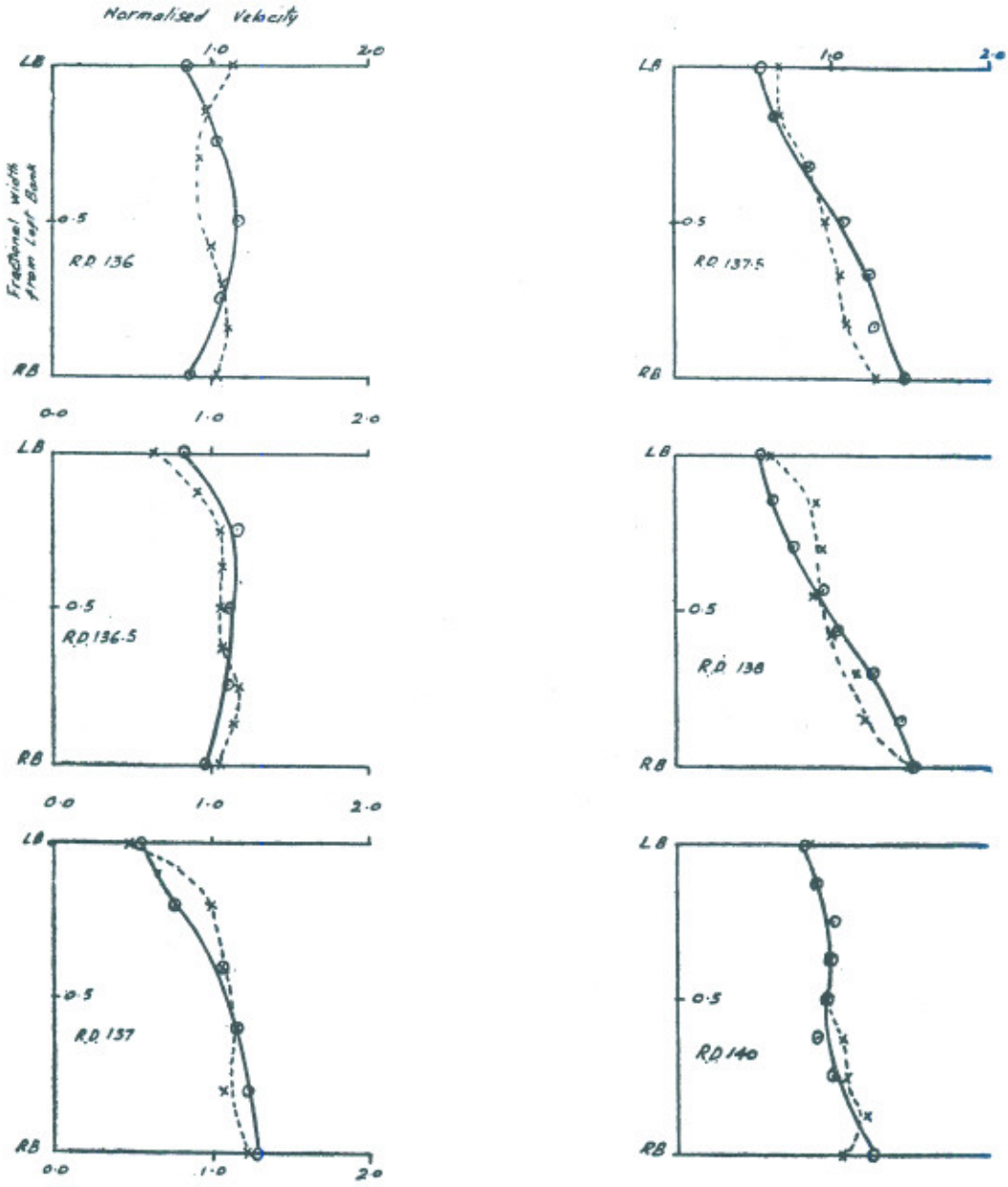

INDEX

Discharge 12000 Cs —o—

Discharge 8000 Cs --x--

Note:- In these diagrams abscissa is average vel in each vertical divided by avg velocity is section

Ordinate is fractional distance from Left Bed Line

FIG. 12·5

LCC COMPLEX

MODEL PERFORMANCE

OF

EQUIANGULAR SPIRAL CURVE

$r = ae^{m\theta}$

(Super elevation in Bed- NIL)

NORMALISED VELOCITY DISTRIBUTION IN SECTION

The effect of sloping the channel bed, across the width would be to decrease the discharge intensity on the outer bank from that without the superelevation. There is no method presently available (even for circular curves) of computing the superelevation that would equalise the discharge intensity distribution in bends. In fact this is generally, not an objective in channel design. It was therefore decided to try arbitrary values of superelevation, so as to determine the amount which would improve the conditions observed at 5,000 cusecs without deteriorating the conditions for higher discharges. Two superelevations of the bed were tried, on the model; one of 2.5 feet and the other of 1.25 feet. In both cases, the bed was raised and lowered on opposite sides by one half of the amount of superelevation and the maximum change in the bed was effected uniformly in a short distance starting from downstream of the Aqueduct. The superelevation was thereafter linearly reduced to zero at the end of the curve.

The velocity data were observed for each of the superelevations as before. It was found that the effect of superelevation was to improve the velocity distribution for 12,000 and 8,000 cusecs discharges and for these conditions there was not much to choose between the two values. The normalised velocity ratio distribution curves for the two superelevations for these discharges are given in Figures 10.6 and 10.7. The velocity distribution at R.D. 140 for all the three conditions of the spiral (Superelevation 2.5 and 1.25 and 0.0 feet) and for the original circular curve are depicted in Figure 10.8 and 10.9 for discharge of 8,000 and 12,000 cusecs respectively. The improvement in velocity distribution with the spiral is apparent.

For 5,000 cusecs discharge, the condition of zero velocity around R.D. 138, was also rectified by both the superelevations equally well. However it was noticed that for the higher value, the flow at the end of the curve (RD 138+) tended to be too close to the left bank. A value of 2.5 feet was thus considered to be over-correcting and the value of 1.25 feet superelevation of the bed at R.D. 136 (linearly diminishing along the curve) was therefore adopted. This also gave a more uniform velocity distribution for all the stages at R.D. 140 (Figures 10.9 and 10.9) and specially for 5,000 cusecs all along the flow. The velocity distribution for this discharge at R.D. 140 for the two superelevations is shown in Figure 10.10.

The equiangular spiral, with a maximum superelevation of the bed of 1.25 feet was accordingly recommended for adoption as the turning-*cum*-expansion transition for the relocated reach of LCC Upper between Aqueduct and Sagar Regulator.

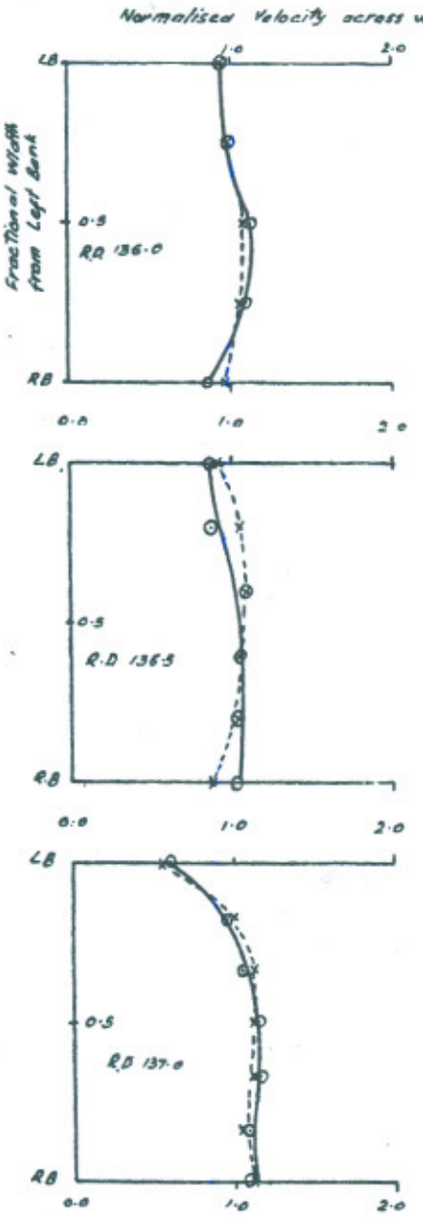

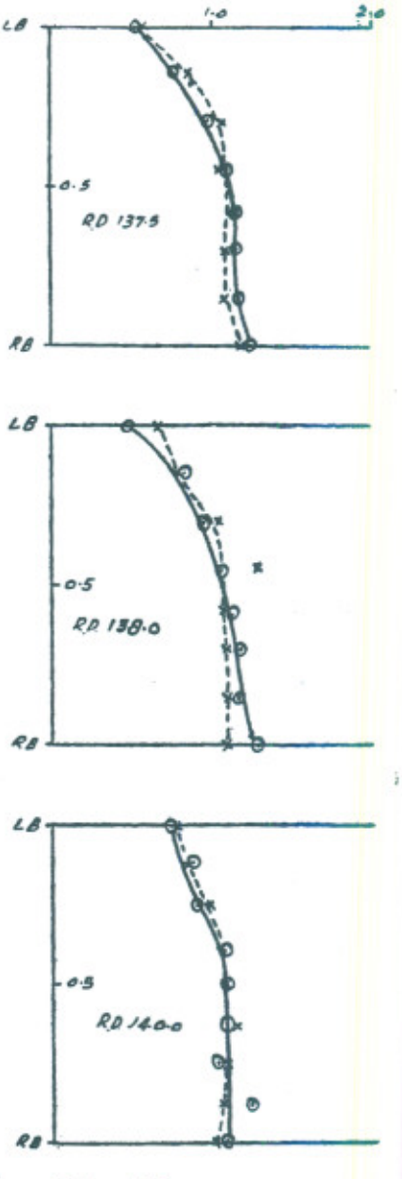

FIG 10·6

LCC COMPLEX
MODEL PERFORMANCE
OF
EQUIANGULAR SPIRAL
(superelevation Max 2·5')
See text

NORMALISE VELOCITY DISTRIBUTION IN SECTIONS

INDEX

Discharge 12000 Cs —o—

Discharge 8000 Cs --x--

Note: In these diagrams abscissa is average vel in each vertical divided by avg velocity is section

Ordinate is fractional distance from Left Bed Line

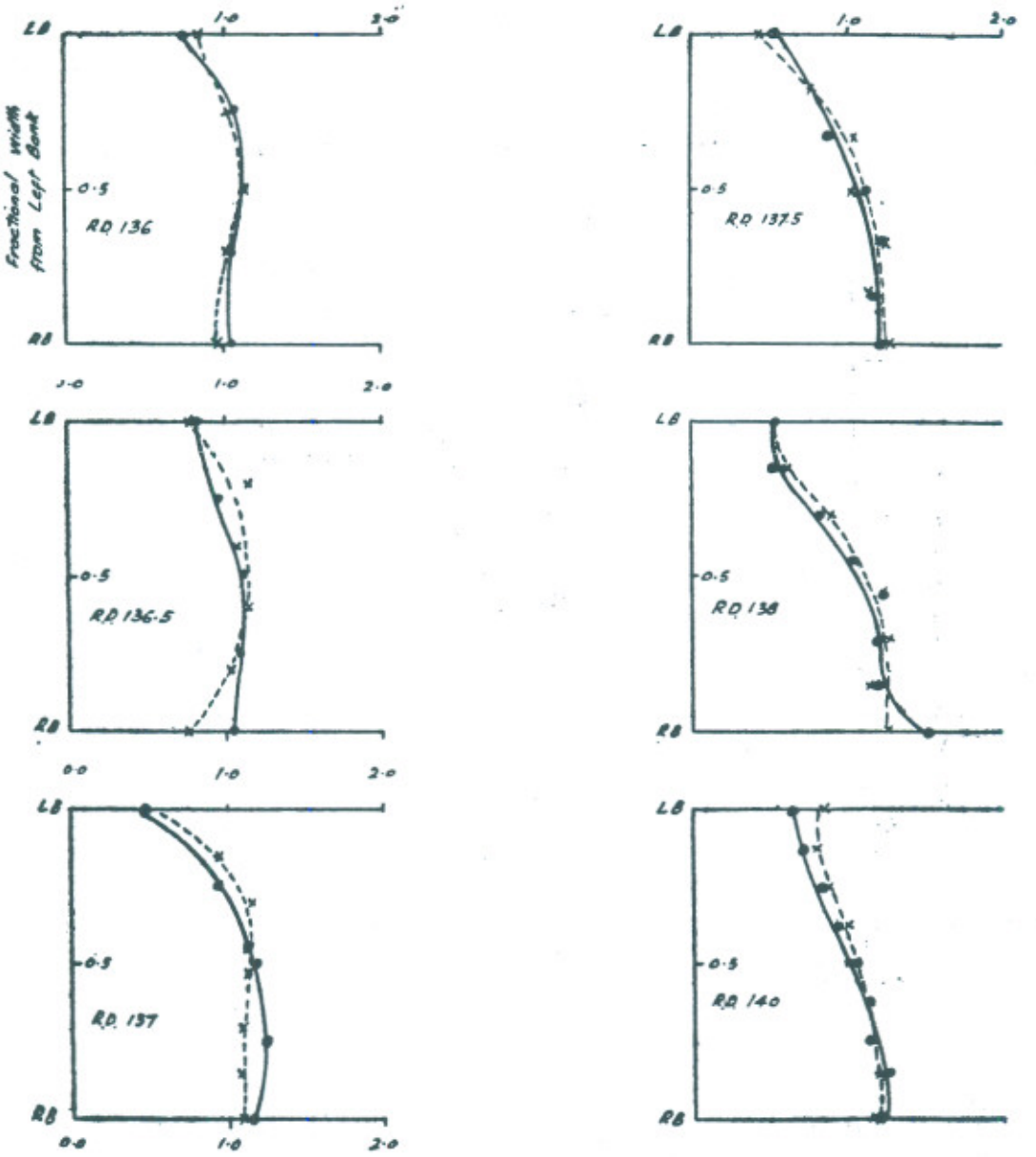

INDEX

Q = 12000 Cs —•—

Q = 8000 Cs. --x--

Note: In these diagrams obscissa is average vel in each vertical divided by avg velocity is section
Ordinate is fractional distance from Left Bed. Line

FIG: 10·9

LCC COMPLEX
MODEL PERFORMANCE
OF
EQUIANGULAR SPIRAL
(Superelevation 1·35)
See Text

NORMALISED VELOCITY DISTRIBUTION IN SECTIONS

B.D. 14a+000

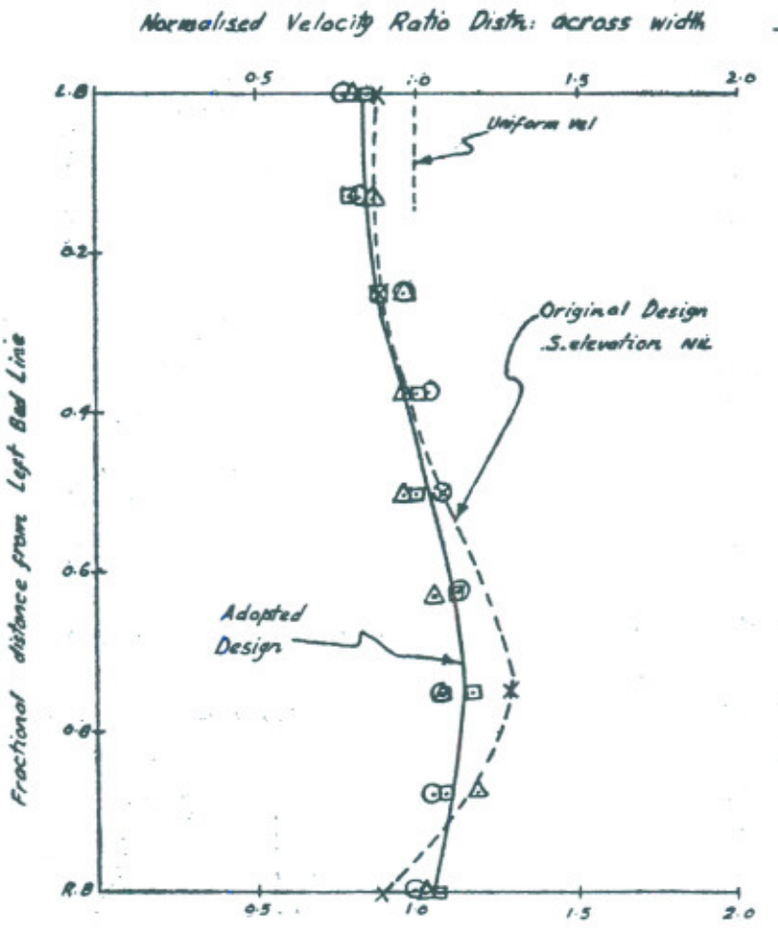

FIG 10.8

INDEX

Bed Superelelevation	2.5'	○
" "	1.25	□
" "	0.00	△
Original Design	0.00	×

LCC COMPLEX

Model Performance of Equiangular Spiral

Q = 8000 Cusecs

R.D. 140+000

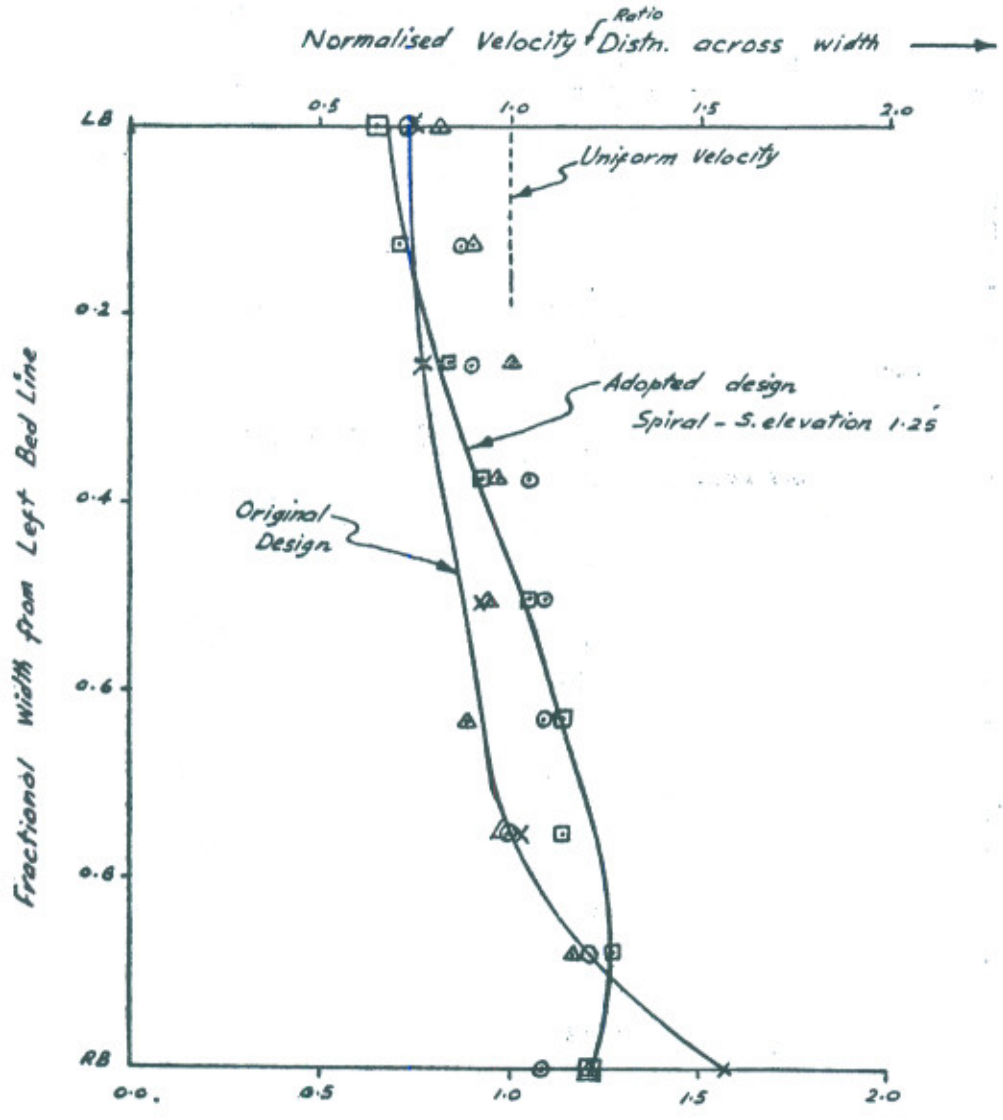

INDEX

Bed Superelevation	2·50	⊙
" "	1·25	⊡
" "	0·00	▲
Original Design	0·00	X

FIG 10.9

LCC COMPLEX

MODEL PERFORMANCE OF EQUIANGULAR SPIRAL

Q = 12000 Cs.

R.D. 140+000

R.D. 140 + 000

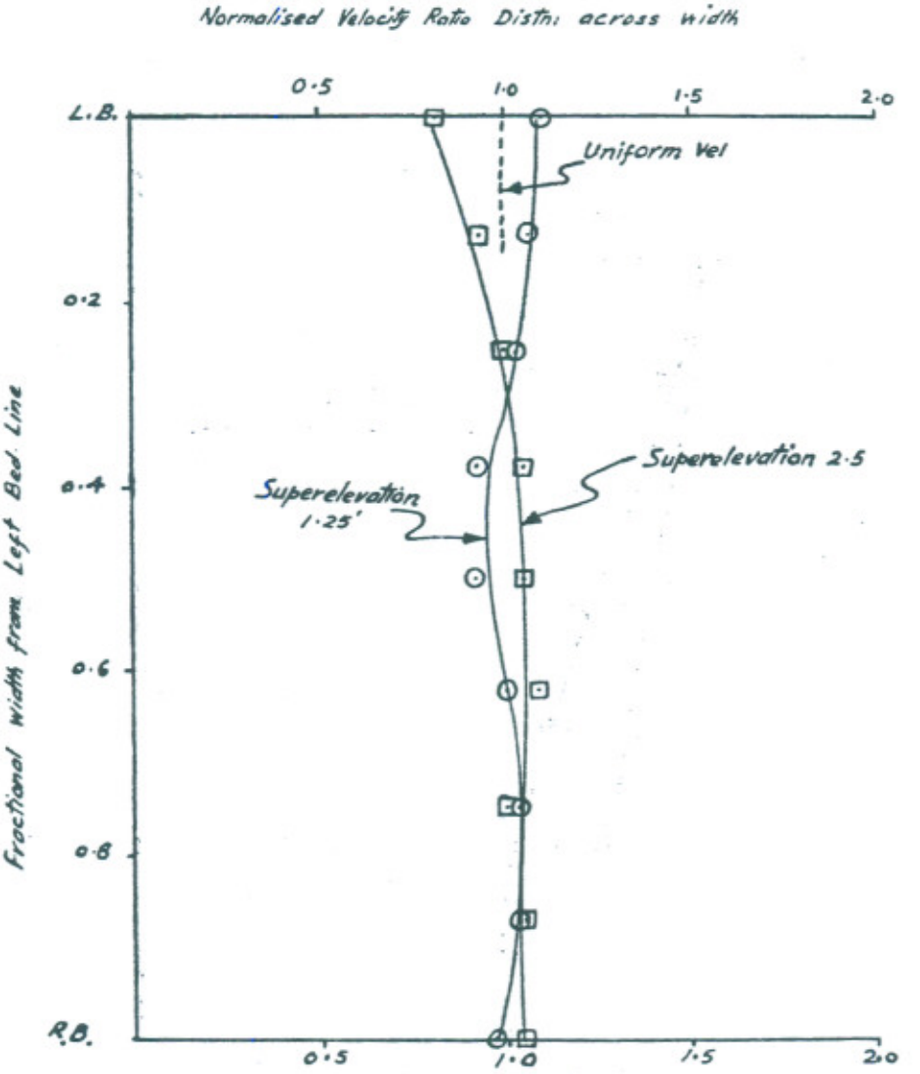

INDEX

Bed Superelevation	1·25	⊙
" "	2·50	⊡

FIG: 10·10

L.C.C. COMPLEX

MODEL PERFORMANCE OF EQUIANGULAR SPIRAL

Q = 5000

11. PROTOTYPE PERFORMANCE OF SPIRAL

The equiangular spiral, as calculated in part 9 and given in Table 9.2, was adopted for construction. Some modification in the curve had to be made to suit changes in alignments of tangents in field. A super elevation of 1.25 feet was provided in the bed. The channel section was lined up to Sagar Regulator with double tile lining. This lining was of standard specification but without the water proofing bitumen layer. In addition to the lining, a two feet high hump was provided at 107 feet upstream of the Aqueduct. A similar hump was provided just after the termination of the spiral (R.D. 138+300). The bed level of the Aqueduct, was also raised from R. L. 690.50 to 690.75, so that the design water level at its downstream end for 8,000 cusecs stage was lowered from 699.70 to 698.86. The Froude Number in the Aqueduct correspondingly increased from 0.50 to 0.61.

For a designed depth of 12.78 feet (12,000 cusecs) the pond level at Sagar would be 702.02 on Survey of Pakistan Datum used in the design. (The Irrigation Datum, at this point is 1.40 feet higher than this). The actual pond maintained at Sagar has varied from 696.84 (SPD) for 6072 cusecs to 698.04 (SPD) for 9,745 cusecs and 700.01 (SPD) for 11,930 cusecs. The pond level at Sagar was maintained as the minimum required for feeding the canals to avoid any heading up in L.C.C. Upper, upstream of relocated stretch. This had accordingly resulted in lower depth in the reach from Sagar to the Aqueduct and in the Aqueduct itself.

In order to evaluate the performance of the spiral, on the prototype, velocity observations were got made at R.Ds. 138+700, 139+330 and 140+500, through the Project Director, Surface Water Hydrology, Wapda. The hydraulic data as observed are given in Table 11.1. The velocity data, in normalised velocity distribution diagrams are shown in Figure 11.1 Computations of energy gradient in the relocated reach downstream of Aqueduct are given in Appendix 'A'. It may be seen that the Froude Number of the flow in the Aqueduct works out to 0.88. Also the value of Mannings 'n' for the straight reach works out to 0.0197 (against 0.020 assumed in design). For the reach R.D. 135+850 to 138+700, which contains the spiral, the energy gradient has a value of 1/4320 against 1/6920 in the straight reach. (The value of 'n' works out inexplicably low). It shows that the spiral has not introduced any extra-ordinary energy losses in the expansion-*cum*-turning transition of the spiral.

The model velocity observations were made at R.D. 140. The normalised model data at this section are also plotted in Figure 11.1 on the prototype diagram for R.D. 140+500 for comparison. In this connection, it is to be noted that the average depth observed in the centre of the channel was 11.3 feet on the

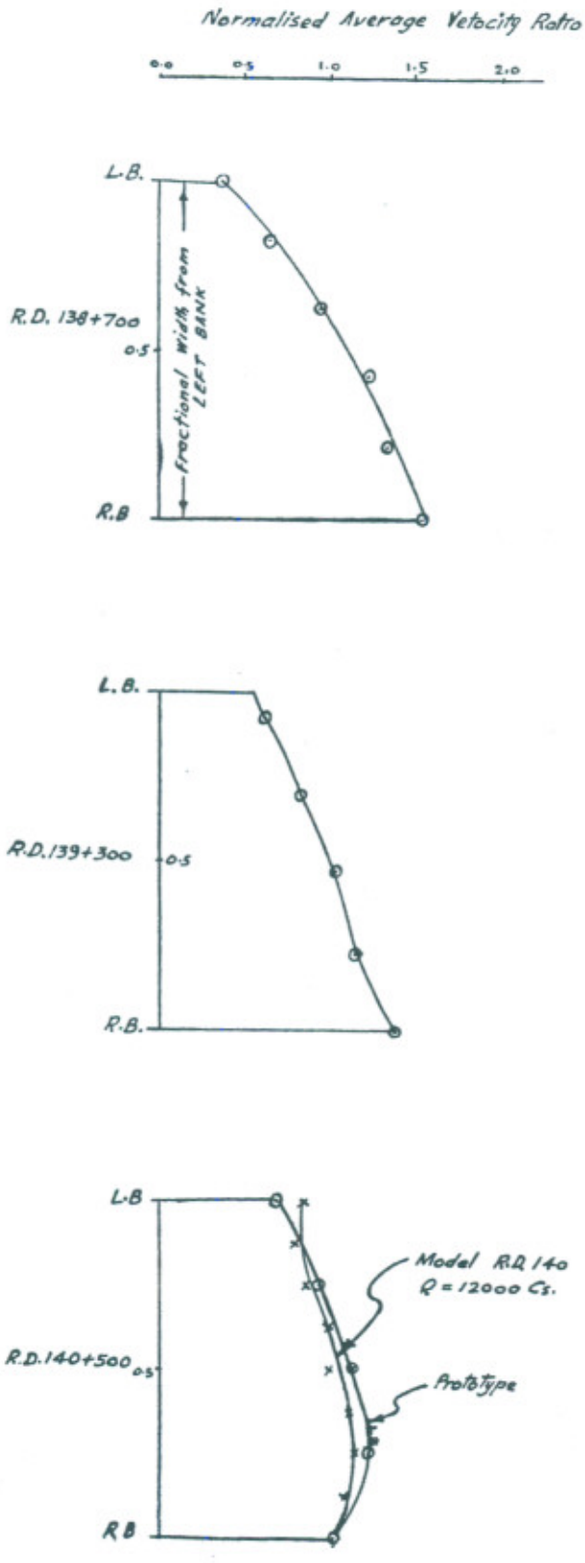

FIG. NO: 11.1

L.C.C. COMPLEX

Relocated L.C.C. Upper

Normatised Average Velocity Ratio

Observed on prototype

Q = 12,400 Cusecs

Date= 20.21 Sept 1967.

prototype, which is about 1.5 feet lower than the designed depth of 12.78 feet. This draw down is because of lower than the designed pond level maintained at Sagar. The discrepancy between the model and prototype velocity distribution is most probably due to this.

The prototype for 12,400 cusecs discharge, showed an excessive wave generation in the Aqueduct, which travelled all the way in the spiral. This was because of the high Froude Number of the flow (0.88) generated in the Aqueduct. If the design conditions are maintained in the Aqueduct (Froude No. 0.61 for 12,000 cusecs). The waves would reduce (though cannot be entirely eliminated). The maintenance of the design pond level at Sagar would also reduce the variation of velocity distribution across the section, in the spiral as well as in the straight reach. The opinion of the Link Canals Directorate of Wapda, was obtained about the performance of the spiral. They had found the transition to be entirely satisfactory.

L.C.C. Upper, was closed in January 1968, and the transition was inspected to see if any shoal formation had taken place. It was found that from R.D. 137+200 to R.D. 138+330, a small sloping shoal, about 2 feet average height and of 30 feet average width had deposited on the inner bank. This shoal can be explained by the lower pond level maintained at Sagar.

During the study of the problem, when the design of the spiral curve was being worked out, certain scepticism was expressed about the possibility of its use. These doubts were mainly based on the reasoning that the spiral curve created a sharper turning than the circular curve in the beginning, where the velocity was also higher and as such it would be more susceptible to separation than the circular curve of the original design. Some concern was also expressed about the "Complicated" nature of the spiral. The spiral design was however adopted on the basis of its model performance. Explanation is now due, on both these points and is offered in the following paragraphs.

As a recapitulation, the following summary of the behaviour of flow in open channel bends is given:

(*i*) The curvature of streamlines on approaching a bend commences in the straight reach and within the curve the curvature is such that at the beginning it is more than, and at the end, less than the curvature of the physical bend.

(*ii*) A superelevation of the free surface develops at entry to the bend and persists throughout the flow in the curve. At the physical end of the curve, the superelevation vanishes almost abruptly. The superelevation, both by its creation and vanishing, brings about a redistribution of velocities in the cross-section. This is

such that with the appearance of superelevation, the flow tends to concentrate on the inner bank and with the disappearance on the outer bank.

(*iii*) In subcritical flow through a curve, separation is possible at two points; along the outer bank just at the entry to the curve and along the inner bank at or about the apex of the curve (where the main flow switches over the opposite bank). It is not possible to analytically forecast whether separation will take place. However it is noted that the depth: bed width ratio is an important factor along with the bed width: radius of curvature ratio. More important than those is the side slope of the channel. It has, for example, been observed that for a channel curve as sharp as bed width: centre line radius of curvature ratio of unity and shallow depth, no separation is noted for vertical banks.

With these generalised ideas, it will be shown as to how the spiral is superior to a circular curve for transitions like these.

TABLE 11.1

SURFACE WATER HYDROLOGY, WASID, WAPDA
L. C. C. COMPLEX—BEHAVIOUR OF SPIRAL TRANSITION

Sr. No.	Date	RD	Q	A SQ.Ft.	Average V Ft/SEC	Surface width Ft.	W. S. Elevation S.P.D.	Wetted perimeter (P) Ft.
13	20-9-1967 &	135+850					698.73	
	21-9-1967	136+500					700.69	
		137+800					700.85	
		138+700		2510*		283	700.86	290
		139+300		2820		283	700.70	289
		140+500	12400	2920	4.25	283	700.62	289

Note: (1) Work finished in two days. There was no change in discharge during the period.

(2) Upper three X-section could not be observed due to high velocities and wave action.

(3) *Two verticals near the right bank could not be observed due to curvature of canal giving cross-drag to the boat.

(4) Water surface elevations taken along left bank.

The radius of curvature of equiangular spiral at any point is given by equation 8.2. For the designed spiral, this works out to 1047 feet for the centre line at the commencement and 2,400 feet at the end of the spiral. The radius of curvature of the circular curve was 1,150 feet. It would thus be seen that the spiral offers a radius of curvature about equal to the circular curve at the beginning but more than double at its end. This should reduce the chances of separation within the bend. At the entry to the curve, the original design provided side slope of 2: 1. The adopted design provided vertical sides, flaring out to 2: 1 slope in a length of about 300 feet. The chances of separation at the entry to the curve are thus considerably reduced.

Another factor creating adverse pressure gradient would be the expansion transition downstream of the Aqueduct. In the circular curve layout of the original design the bed width is flared out from 110 to 240 feet at an effective flaring out of 1 in 4 on both the sides (Figure 3.3). In the spiral, as is shown in Appendix B, the rate of expansion is constant throughout and effectively works out to 1 in 40. The rate of rise of flow depth has also been calculated in Appendix B, to show that the total adverse pressure gradient at the commencement of the spiral (including that due to superelevation) is three-tenth of that due to the expansion transition alone. Thus the spiral would present lesser chances of separation at the entry to the transition. As the radius of curvature of the physical bend in spiral is shorter at the beginning, it also conforms more to the natural behaviour of streamlines that a circular curve.

Another superiority of the spiral over the circular curve is the increased radius of curvature at the downstream end. It has already been stated, that the disappearance of superelevation causes a readjustment of velocity distribution in the section and that it draws the maximum velocity isovel more to the outer bank. Also it can be analytically shown that more is the superelevation at the end, the greater will be the enhanced concentration of velocities on the outer bank at the end of the curve. The superelevation for the circular curves is constant at about 0.1 foot for 12,000 cusecs discharge. For the same discharge in the spiral, it reduces from a maximum value of 0.3 at the beginning to 0.05 feet at the end. It would thus be seen that given other factors equal, the velocity distribution at the end of spiral would be comparatively more uniform than that at the end of circular curve. It may also be noted here, that in prismatic open channels (with unchanging area of cross section), the transitions between the main curve and the tangent lengths are provided in the shape of curves of double the radius of the main curve. The effect of these curves is to split the superelevation at the outfall into two steps and hence improve the velocity distribution in the section. It is thus seen, from the characteristics

of the flow in open channel bends, that for expansion-*cum*-turning transitions an equiangular spiral is superior to contiguous expansion and turning transitions (unless equilising straight reaches of adequate length can be introduced in between the two).

About the complicated nature of the curve or its equation, the analysis of the properties of equiangular spiral and the geometrical methods of construction would show, that the methods of layout are not difficult and on the other hand lend themselves to easy geometric construction. It is hoped that these methods, which were evolved, during the design of spiral for LCC Upper, will help in a solution of similar problems in future.

12. CONCLUSION

On the crossing of Qadirabad-Balloki Link and LCC Upper, the conditions of engineering design had dictated a combination of sharp expansion and a sharp channel curve. Hydraulic model testing of the proposed design indicated that separation of flow occurred over a major part of the curve.

An equiangular spiral represents the stream lines from a two dimensional source of steady strength superimposed by a vortex of steady circulation. These streamlines turn and expand simultaneously. After a number of corrective devices and channel realignment proposals had been found unsuccessful, an equiangular spiral transition was calculated and fitted between the aqueduct and the relocated LCC Upper. This curve was found suitable as it obviated separation of flow from solid boundaries and also yielded a more uniform velocity distribution across the section, in the straight reach downstream of the curve. For further improving the velocity distribution at low stages, a superelevation of 1.25 feet across the channel bed at R.D. 136 was found adequate. This was accordingly recommended as an alternative to the original design and was adopted for construction at site with minor modifications needed because of further realignment of the tangent reaches.

The properties of the equiangular spiral have been analysed in this paper and methods of geometrically and analytically fitting the equiangular spiral between two tangents have been described.

The model study, of the original design and the equiangular spiral, has been discussed. The derivation of model scale ratio and the errors involved in scaling off various characteristics of flow in bends have also been discussed to show as to how such limitations of small scale model studies can be visualised and accounted for.

The prototype of the spiral has since been constructed at site and run for about one year till now (January 1968). The prototype spiral does not show

any separation of flow from solid boundaries. Because of the high Froude Number of flow in the Aqueduct (0.50 for 12,000 cusecs) the surface of the flow is unstable and waves thus generated travel throughout the spiral. Prototype data has been got observed for a discharge of 12,400 cusecs, which shows depths upstream of Sagar are less than those assumed in design. The excessive wave generation presently noted in the field is due to the lower pond levels maintained. The Manning 'n' for the straight reach in the prototype works out to be the same as assumed in the design. Also the spiral does not seem to be causing any extra-ordinary energy loss. Velocity profiles observed downstream of the spiral have been analysed and compared at one section with the model data, which show reasonable correspondence.

The flow characteristics in the open channel curves have also been briefly discussed and it is deduced as to how the spiral transition is better than contiguous expansion and turning transitions.

Flow in open channel curves is important in the design of rigid boundary channels. It is all the more important in alluvial channels and the behaviour of meandering river channels. In the Irrigation practice in West Pakistan, the limiting radii of alluvial channels are conservatively fixed. It is believed that considerable knowledge about the flow in the channel curves can be obtained by a detailed hydraulic and sediment data observation program on the existing canal curves. In the meandering rivers it is noted that direction of curvature is changed by the natural rivers over fairly short reaches. This phenomenon is also related to some transition curves introduced naturally. Data on meandering rivers if observed for the distribution of longitudinal and radial velocities, distribution of discharge, sediment grade and sediment transport in the sections, limiting depths on the convex bends etc. etc. can provide improved insight in the mechanism of these channels. A study on the effect of various transition curves on the limiting radii of circular curves in alluvial channels can also be helpful in improving the design practice.

REFERENCES CITED

2.1 "Design Report on Qadirabad-Balloki Link Canal" Tipton and Kalmbach, Inc., Engineer, Lahore, January 1963. Volumes I and II.

3.1 Rozovskii, I. L., "Flow of water in Bends of Open Channels", Academy of Sciences of the Ukrainian SSR, Kiev, 1957. English translation distributed by Oldbourne Press, London.

7.1 Streeter, Victor L., "Fluid Mechanics", McGraw Hill Book Company Inc., New York, 1962.

APPENDIX 'A'

COMPUTATION OF ENERGY GRADIENT OBSERVED ON RELOCATED L C C UPPER

Q = 12400 cusecs
R.D. 135 + 850
Depth = 7.98 ft.
Width = 110 ft.

$V = \frac{12400}{7.98 \times 110} = 14.1$ ft./sec. $F = \frac{14.1}{32.2 \times 7.98} = 0.88$

$\frac{V^2}{2g} = 3.09$ ft.

R.L. TEL = 698.73+3.09 = 701.82

R.D. 138+700
Area = 2820 ft.^{2}

Velocity $= \frac{12400}{2820}$ = 4.4 ft./sec.

$\frac{V^2}{2g} = 0.30$ ft.

WSL = 700.86
R.L. TEL = 700.86+0.30 = 701.16

R.D. 140+500
Area = 2920 ft.^{2}

Velocity $= \frac{12400}{2920}$ = 4.25 ft./sec.

$\frac{V^2}{2g} = 0.28$ ft.

WSL = 700.62
R.L. TEL = 700.62+0.28 = 700.90

Total Energy gradient

(*i*) R.D. 135+850 to 138+700
Length = 2+850
ΔE = 701.82—701.16 = 0.66 ft.

$\frac{\Delta E}{L} = \frac{0.66}{2850} = \frac{1}{4320} = 0.232 \times 10^{-3}$

(*ii*) R.D. 138+700 to R.D. 140+500

Length = 1+800

ΔE = 701.16 — 700.90 = 0.26 ft.

$\frac{\Delta E}{L} = \frac{0.26}{1800} = \frac{1}{6920} = 0.145 \times 10^{-3}$

(*iii*) R.D. 135+850 to R.D. 140+500

Length = 4+650

ΔE = 701.82—700.90 = 0.92 ft.

$\frac{\Delta E}{L} = \frac{0.92}{4650} = \frac{1}{5050} = 0.198 \times 10^{-3}$

(*iv*) Extra $\frac{\Delta E}{L}$ for spiral curve including transition

Reach 135+850 to 140+500 $(0.198—0.145) \times 10^{-3} = 0.053 \times 10^{-3}$

Reach 135+850 to 138+700 $(0.172—0.145) \times 10^{-3} = 0.027 \times 10^{-3}$

(*v*) Manning '*n*'

Reach R.D. 138+700 to 140+500

A = 2920 ft.^{2}

P = 289 ft.

$R = \frac{2920}{289} = 10.1$ ft.

$R^{2/3} = 4.67$

$S = \frac{1}{6920}$

$S^{1/2} = \frac{1}{83.1}$

V = 4.25 ft./sec.

$n = \frac{1.49 \times 4.67}{4.25 \times 83.1} = 0.0197$ against 0.020 (design)

APPENDIX 'B'

COMPUTATIONS OF SOME HYDRAULIC CHARACTERISTICS OF FLOW IN EQUIANGULAR SPIRAL

(1) Superelevation of Free Surface

Equiangular spiral

Radius of curvature of any point,

$$\rho = \frac{r_0}{\text{Sin } \alpha} \qquad \text{Equation 8.2}$$

Sin $\alpha = 0.8859$

(*a*) Discharge 12,000 cusecs.

(*i*) At beginning of spiral

radius vector to centre line $roa \cong 927$ ft.

$\rho oa = 1047$ ft.

Top width = 110 feet.

Average velocity = 9.58 ft./sec.

Superelevation $= \frac{V^2 B}{g \rho_o} = 0.30$ feet.

(*ii*) At end of spiral

roc	= 2123 feet.
ρoc	= 2400 feet.
Top width	= 290 feet.
Average velocity	= 3.54 feet/sec.
Superelevation	= 0.047 feet.

(*b*) Discharge 8,000 cusecs.

(*i*) At beginning of spiral

Average velocity	= 7.90 ft./sec.
Superelevation	= 0.204 ft.

(*ii*) At end of spiral

Average velocity	= 3.08 ft./sec.
Superelevation	= 0.036 ft.

Circular curve Radius 1150 feet.

(*a*) Discharge 12,000 cusecs.

Average velocity	= 3.54 ft./sec.
Superelevation	= 0.098 feet.

(*b*) Discharge 8,000 cusecs.
Average Velocity = 3.08 ft./sec.
Superelevation = 0.076 feet.

2. Adverse Pressure Gradient due to Superelevation

Assuming full superelevation is developed in a length of about 100 feet (same order as width of flow in aqueduct) Adverse pressure gradient for the spiral and circular curve are as below

Adverse pressure gradient

Point	Spiral		Circular Curve	
	Discharge 8,000 cusecs	Discharge 12,000 Cs.	Discharge 8,000 Cs.	Discharge 12,000 Cs.
Beginning of curve ..	0.002	0.003	0.0008	0.0010
End of curve ..	0.0004	0.0005	0.0008	0.0010

3. Adverse Pressure Gradient due to Widening of Bed

The bed width of the channel from 110 feet at aqueduct to 240 feet at canal section is changed in two ways. In the spiral the bed width continuously increases along the length, while in the circular curve, it is first increased to 240 feet in the flaring out transition and then remains constant in the curve. In open channel flow, the change in the bed also changes the depth of flow. The increase in bed width is accompanied by increase in depth (subcritical flow). Since the pressure distribution remains hydrostatic even for considerable curvature of streamlines, the rate of change of depth with distance along the centre line represents adverse pressure gradient. It will first be shown that in equiangular spiral, the rate of increase of bed width is constant all along the length of the curve and is independent of the position along the curve.

(*a*) Rate of change of Bed width along centre line

Bed width $B = (r_2 - r_1) \sin \alpha$

Where r_2 and r_1 are the radius vectors to the outer and inner edges of the spiral, and $\alpha = \cot^{-1} m$.

Length of curve along centre line, between points 2 and 1,

$$S_{2-1} = \frac{ro_2 - ro_1}{\cos \alpha}$$

Where ro_2 and ro_1 are the radius vectors to points 2 and 1 on the centre line spiral curve.

Then $B = (r_2 - r_1) \sin \alpha$

$$= (a_2 - a_1)\, e^{m\theta} \sin \alpha \qquad ..B.1$$

$$ds = \frac{dro}{\cos \alpha} \qquad ..B.2$$

Where a_2 and a_1 are length of radius vectors for outer and inner edge spirals for $\theta = 0$, ds = finite increment of length along centre line, for a finite increment *dro* of the radius vector to centre line spiral.

Now $$\frac{dB}{ds} = \frac{dB}{d\theta} \cdot \frac{d\theta}{dro} \cdot \frac{dro}{ds}$$

From equation B.1

$$\frac{dB}{d\theta} = (a_2 - a_1)\, m. \sin \alpha\, e^{m\theta}$$

From equation of spiral

$$\frac{dro}{d\theta} = mao\ e^{m\theta}$$

From equation B.2

$$\frac{dro}{ds} = \cos \alpha$$

Therefore $\frac{dB}{ds} = \frac{(a_2 - a_1)}{ao} \cos \alpha . \sin \alpha$, which is only dependent on the parameters of spiral and not on location of point

Now $(a_2 - a_1) \sin \alpha$ is also equal to the normal width of channel at the beginning of the transition and $a_0 = 977$

$$\frac{dB}{ds} = \frac{110}{977} \times 0.4643 = 0.0522 \qquad ..B\text{-}3.$$

(*b*) Rate of change of Depth with increasing Bed width (Sub-critical flow)

In rectangular channels, the Specific Energy E, is given by

$$E = \frac{Q^2}{2g\, B^2 d^2} + d \qquad ..B\text{-}4.$$

Where Q = total discharge, B is the bed width and d is the depth of flow.

Differentiating equation B-4. with respect to S the length along centre line of flow

$$\frac{dE}{ds} = \frac{Q^2}{2g} \left(\frac{-2}{B^2 d^3} \frac{dd}{ds} - \frac{2}{B^3 d^2} \frac{dB}{ds} \right) + \frac{dd}{ds}$$

Assuming the bed slope of the channel equal to the energy gradient,

$\frac{dE}{ds} = 0$ The expression can thus be arranged as

$$\frac{dd}{ds} = \frac{d}{B} \frac{2(E-d)}{(3d-2E)} \frac{dB}{ds} \qquad ..B.5$$

In equation B.5, the left hand side represents the rate of change of depth with length along centre line and hence the adverse pressure gradient. E, d and B pertain to the point under consideration and $\frac{dB}{ds}$ is the rate of change of bed width along the centre line. For an equiangular spiral $\frac{dB}{ds}$=constant.

(*c*) Adverse Pressure Gradient on Spiral

(*i*) For 12,000 cusecs discharge

At beginning of spiral.

d = 11.4 ft.
V = 9.58 ft./sec.
E = 12.82 ft.
B = 110 feet.
$\frac{dB}{ds}$ = 0.0522 (from equation B-3)
$\frac{dd}{ds}$ = 0.0015

At end of Spiral

d = 12.78 feet.
v = 3.54 feet/sec.
E = 12.98 feet.
B = 240 feet.
$\frac{dB}{ds}$ = 0.0522
$\frac{dd}{ds}$ = 0.0000088 (negligible)

(*ii*) For 8,000 cusecs.

At beginning of curve

d = 9.2 feet.
V = 7.90 feet/sec.
E = 10.17 feet.
B = 110 feet.
$\frac{dd}{ds}$ = 0.0012

At end of spiral, negligible as before.

(*d*) Adverse Pressure Gradient due to Expanding Transition of original design.

The original design bed provided an effective flaring out of bed width of 1 in 4. For this condition.

$$\frac{dB}{ds} = \frac{1}{2} = 0.5$$

and $\frac{dd}{ds}$ is given by equation B.5 as before

For 12,000 cusecs discharge

$$\frac{dd}{ds} = 0.012 \text{ at the beginning of the transition}$$

Now total adverse pressure gradient for spiral for 12,000 cusecs discharge
= due to curvature and due to expansion
= 0.003 + 0.0015 = 0.0045
and for 8,000 cusecs,
= 0.002 + 0.0012 = 0.0032

For circular curve, assuming it is only because of the expansion, it is equal to 0.015 for 12,000 cusecs and 0.012 for 8,000 cusecs.

Also it may be seen, that if the expansion transition downstream of aqueduct had to provide same adverse pressure gradient as the combined effect of expansion plus curvature of spiral, the flaring out had to be at 1 in 13, which would have required about 850′ long expansion transitions.